香港氣象學會

HKMetS BULLETIN, Volume 3, Number 2, 1993

HONG KONG METEOROLOGICAL SOCIETY

BULLETIN

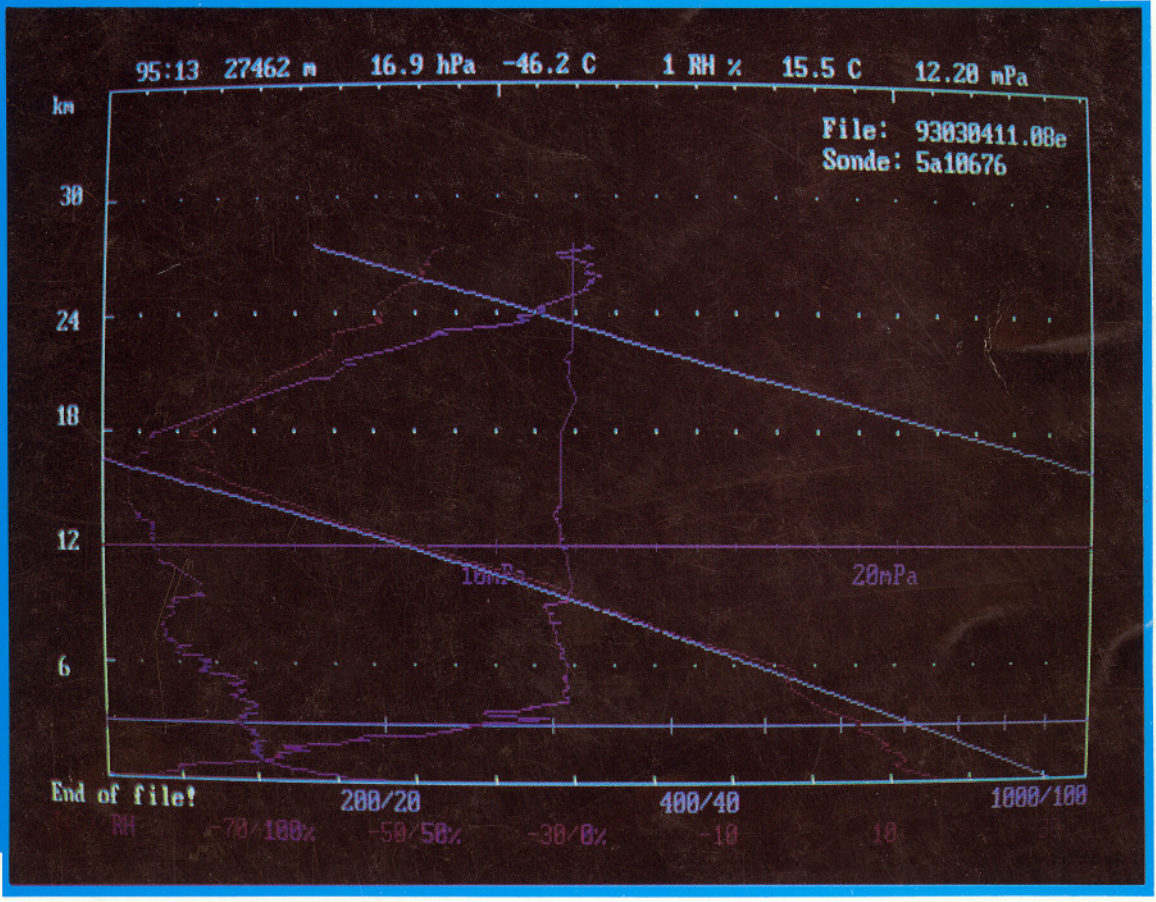

香港氣象學會

HKMetS BULLETIN, Vol. 3, Number 2, 1993

HONG KONG METEOROLOGICAL SOCIETY

BULLETIN

CONTENTS

Editorial 2

Recent Sea-Level Changes in Hong Kong and Their Implications 3
Wyss W.S. Yim

Diurnal Atmospheric Secondary Circulations over Hong Kong 9
Mickey Man-Kui Wai

The First Radioactivity and Ozone Soundings in Hong Kong 21
C.M. Shun & K.S. Leung

News and Announcements 28

Hong Kong Weather Reviews 39

Meeting Reviews 45

Editorial

This issue of the *Bulletin* has, like its predecessor, been somewhat delayed in its publication primarily as a result of the heavy workload of the Editorial Board. We apologize for this but hope that despite the delay you will consider that the quality of the papers provided will more than make up for the extra waiting time. We would like to thank the authors, too, for bearing with us during this time.

The first paper in this issue, by W.W.S. Yim of The University of Hong Kong returns to a subject dealt with in an earlier *Bulletin*, sea-level change. In his paper *Recent Sea-Level Changes in Hong Kong and Their Implications* Dr. Yim analyzes sata collected from tide gauges in Hong Kong and shows that the Hong Kong area is undergoing uplift at a rate of about 1 mm/year. He then examines the implications of this in terms of long term ground settlement, particularly in coastal reclamations, and the impact of sea-level rise on coastal development planning in Hong Kong.

In the second paper Dr. Mickey M.K. Wai of the Florida State University examines the *Diurnal Atmospheric Secondary Circulations over Hong Kong*. The paper shows that these are primarily generated by the sea-land surface temperature difference and as such the secondary circulation behaves like a sea-land breeze.

The third paper, by C.M. Shun and K.S. Leung reports on *The first Radioactivity and Ozone Soundings in Hong Kong*. This report describes the instruments and the ascents which have provided the very first upper-air radioactivity and ozone data sets for Hong Kong. Future plans for carrying out radioactivity and ozone soundings are also described.

The rest of the *Bulletin* continues the same format of previous issues with the regular features *News and Announcements*, *Hong Kong Weather Reviews*, and *Meeting Reviews* all included. The *News and Announcements* section includes several articles originally posted on the Internet which we hope will be of interest to readers. These include forecasts for 1993 Atlantic Hurricane Season Activity and Sahel Rainfall made by Colorado State University meteorologists. It is hoped to follow up on these forecasts in future issues. Two reports, one on the NASA Topex/Poseidon Mission, and another on a meeting held in Melbourne, Australia on Climate Change and ENSO are also included.

The Editorial Board hope that you find this issue interesting and useful. Your support for future issues is always sought in the form of contributions of either papers or correspondence.

Bill Kyle, Editor-in-Chief

Wyss W.S. Yim

Department of Geography & Geology

The University of Hong Kong

*Recent sea-level changes in Hong Kong and their implications**

ABSTRACT

An analysis of data collected from tide gauges has indicated that the Hong Kong area is undergoing uplift at a rate of about 1 mm/year. However, in coastal land reclamations under the influence of long term ground settlement, the rate of subsidence may exceed the rate of uplift resulting in an apparent relative sea-level rise. Consequently, reclaimed land affected by large amounts of ground settlement are susceptible to marine inundation during storm surges generated by typhoons. In order to assist future coastal development, it is recommended that continuous monitoring of long term ground settlement is carried out on the reclaimed land using state-of-the-art surveying methods including satellite altimetry and laser ranging. This is needed to provide warning on subsidence problems so that measures including sea defence by dykes and flood pumping stations may be used to address the problem of flood damage.

Introduction

Global warming through increases in energy production is expected to result in a future sea-level rise. The impact of this on densely populated low-lying coastal mega-cities is a matter of universal concern. However, are the global rates of future sea-level rise which are predicted applicable to different parts of the world? In the present study, the local evidence for recent sea-level changes in the city of Hong Kong is reviewed followed by an assessment of the implications.

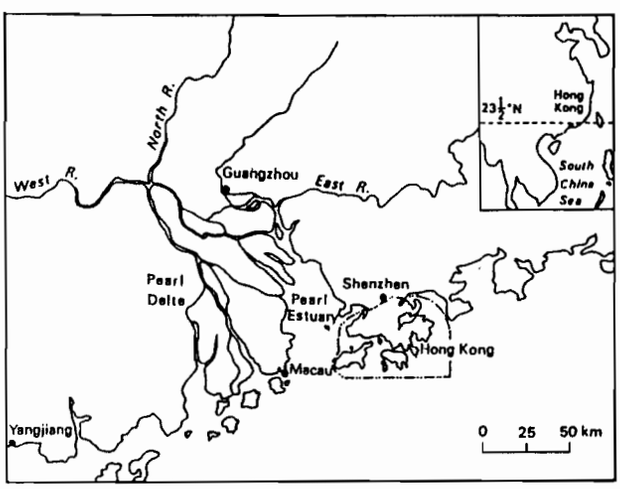

Figure 1 Map of Hong Kong and the Pearl Delta.

Hong Kong is situated near to the mouth of the Pearl River estuary on the northern coast of the South China Sea (Figure 1). Although southern China is regarded as a passive continental margin by Taylor and Hayes (1980), earthquakes up to a Richter scale of 6.4 have occurred within 280 km of the territory at Yangjiang. The western part of the territorial waters of Hong Kong is influenced by discharges from the Pearl River Delta which is advancing rapidly in a southerly direction at an average rate of 50 to 60 m/year (Huang, 1984). The total land area of Hong Kong is about 1,100 km^2 with close to 10 % consisting of coastal land reclamations (Peart and Yim, 1992). It has a total population of just under 6 million with about 60 percent concentrated in the Victoria Harbour area (Figure 2). Because the upland areas are difficult to develop and are prone to landslides, much of the densely populated existing urban areas are

* reprinted from *SEACHANGE '93. Proceedings International Workshop on Sea-level Changes and their Consequences for Hydrology and Water Management, Noordwijkerhout, Netherlands, April, 1993*. Bundesanstalt fur Gewasserkunde, IHP/OHP-Sekretariat, Koblenz, 89-98.

Figure 2 Oblique air photograph of Victoria Harbour showing extensive areas of coastal land reclamations on both sides of the harbour including most of the Kai Tak International Airport.
(Reproduced with permission from the Director of Building and Lands, Hong Kong Government).

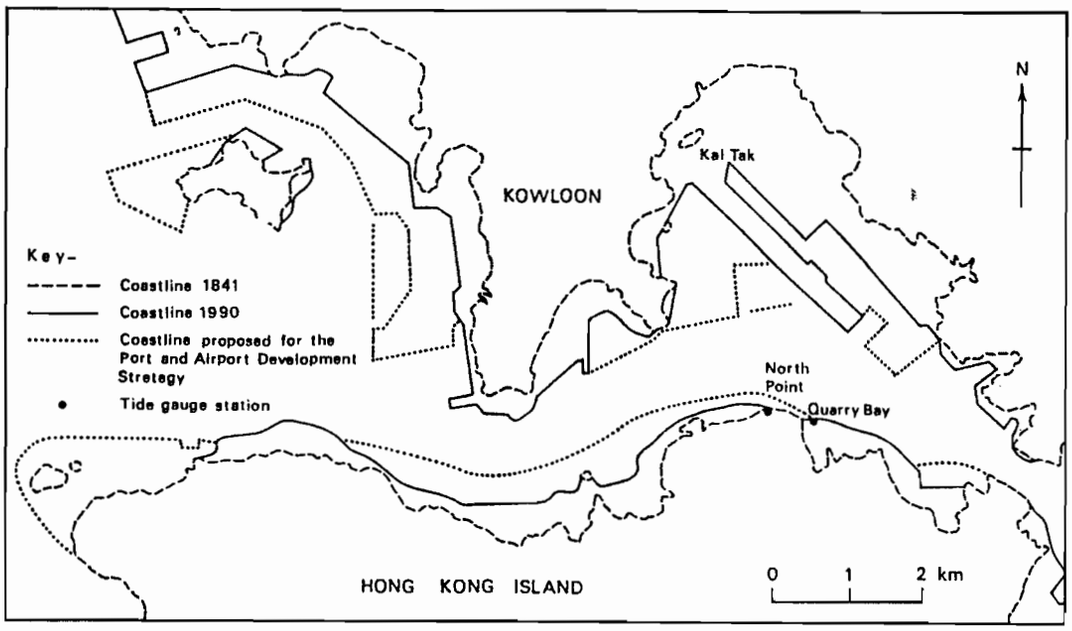

Figure 3 Map of Victoria Harbour showing the position of the coastline during 1841, 1990 and the coastline proposed for PADS. Because the reclaimed land is low-lying, it is prone to flooding during rainstorms and storm surges.

low-lying land created through coastal land reclamations in the past 100 years. Since 1841, dramatic changes of the coastline have taken place within Victoria Harbour (Figure 3). New reclamations are currently being constructed and are being planned for the Port and Airport Development Strategy (PADS). A common feature of the reclaimed land is that it does not normally exceed 6 m above Principal Datum (P.D. - the local reference datum which is about 1.15 m above mean sea level.

Evidence for recent sea-level changes

The evidence for recent sea-level changes in Hong Kong was examined previously by Yim (1991a; 1991b; 1992 and 1993). Based on the results of the analysis of tide gauge stations, Yim (1992) concluded that the ground stability of stations located on coastal land reclamations warranted attention. The longest running tide gauge station at North Point (Figure 3) was operated for 34 years before it was replaced by the Quarry Bay station. Both stations are located on reclaimed land. Surveying checks made on the North Point station and benchmarks from 1954 onwards permitted the correction of sea-level elevations against ground settlement (Yim, 1991a; 1991b and 1992). Between 1954 and 1983, a total settlement of 16.3 cm or a rate of 5.4 mm/year was found (Yim, 1991b). When the average rate of ground settlement is deducted from the annual mean sea level, no rising sea-level trend can be found. Furthermore, if comparisons are made between the corrected annual mean sea levels at the North Point and Quarry Bay stations with other stations in Hong Kong which have been found by check surveying to be unaffected by ground settlement, crustal uplift is indicated. Although the rate of uplift is difficult to quantify accurately, comparison of graphical plots of annual mean sea levels for tide gauge stations with the longest record showed a figure in the region of 1 mm/year (Yim, 1991b). This is similar to the rate of 0.6 mm/year obtained by repeated precise levelling over a 16-year period from 1960-1975 for the Shenzhen area bordering Hong Kong (C. Yang, *personal communication*). Because the North Point and Quarry Bay stations are both located on reclaimed land, the ground has subsided at rates exceeding that of crustal uplift.

High sea levels of short duration are caused by storm surges associated with the passage of typhoons close to Hong Kong. The highest predicted astronomical tide level is only 2.7 m P.D. but the maximum sea level during major typhoons in some parts of the territory may

exceed this elevation by more than 3 m. The elevation of sea level attained at different localities appears to be largely related to the coastal configuration (Yim, 1993). Within the area of Hong Kong, large differences are possible due largely to the irregular natural coastline. During the passage of a typhoon, sea levels at different localities also vary with time as a result of changes in wind direction. The sand bars present in many embayments such as at Pui O on Lantau Island in western Hong Kong can be attributed to a storm beach and/or blown sand origin (Meacham and Yim, 1983). They are considered to be relic features formed by high sea levels associated with storm surges.

Implications

It can be seen from the previous section that notwithstanding the belief that global warming will result in a worldwide future sea-level rise, local factors such as crustal uplift and subsidence must be taken into account for the accurate prediction of sea-level change. In the case of Hong Kong, allowance for the greenhouse effect in engineering design (Kwok, 1990) cannot be justified on the basis of local evidence. The record of tide gauge stations has failed to show a rising sea-level trend but relative sea level has been found instead to be falling due to crustal uplift. However, at least some of the coastal land reclamations was indicated by the North Point tide gauge site to be subsiding through long term ground settlement at rates exceeding crustal uplift. Therefore there is an apparent relative sea-level rise in the areas affected.

Reclaimed land affected by high rates of ground settlement are the most susceptible to marine inundation during storm surges generated by typhoons. This is of the greatest concern in all low-lying coastal areas. In addition to sea flooding, rainstorm flooding resulting from changing hydraulic gradients consequent upon reclamation may also increase the flood hazard (Peart and Yim, 1992). Flooding is also exacerbated by the "trough-effect" created by old reclamations which have settled between the upland areas and the new reclamations which have higher elevations.

Ground elevations of reclaimed land in Victoria Harbour available from topographic maps show many areas including seawalls to be below 4 m P.D. These areas are prone to overtopping by waves and sea flooding during storm surges. The increase in elevation of seawalls to 4.5 m P.D. in the newer coastal land reclamations would provide better protection including the effects of possible long term ground settlement. However, rainstorm flooding is exacerbated because the reclaimed land has very little gradient available for gravity drainage.

According to Yim (1991b) the causes of long term ground settlement in coastal land reclamations are attributable to a wide range of factors including:

1) Diagenetic compaction of soils including the release of gas.
2) Surcharge loading including piling.
3) Blasting through quarrying and tunnelling.
4) Regional and local earthquakes.
5) Mudwaves generated by coastal land reclamations.
6) Tunnelling within coastal land reclamations.
7) Erosion through leakages from water supply and drainage pipes.
8) Excavation particularly when dewatering is carried out.
9) Mass movement generated by the removal of fill deposits on the sea bed.
10) Rapid drawdown.

Coastal land reclamations formed of granular aggregates are susceptible to spontaneous liquefaction induced by earthquakes, blasting and other vibrations particularly when they are not well compacted after emplacement. In addition, when reclamations are extended offshore into deeper waters, a greater thickness of soft marine muds is usually encountered (Yim, 1991c). Because of this, there are likely to be higher rates of long term ground settlement. In order to monitor ground settlement and sea-level changes, it is necessary to make use of state-of-the-art surveying methods including satellite altimetry and laser ranging (known collectively as the global positioning system, GPS) as well as the establishment of new bedrock benchmarks for checking tide gauge levels. Regular check surveying would provide data to permit the estimation of the rate of crustal uplift and the rate of subsidence of tide gauges located on reclaimed land. In Hong Kong, benchmarks founded on bedrock have been installed adjacent to all tide gauges to permit continuous monitoring of possible ground settlement. This installation programme was completed in 1991 (H.H. Choy, *personal communication*). While the use of GPS is under consideration by the Hong Kong Government, some evidence has been found for tide gauge levels to be influenced by moderate scale regional earthquakes (Yim, 1991d). Without GPS, it will not be possible to estimate the rate of crustal uplift accurately.

Conclusions

This study shows the importance of using local evidence for determining recent sea-level changes in Hong Kong. For planning future coastal development, it is misleading to use a global rate of predicted sea-level rise without making adjustments for local rates of uplift and subsidence. Coastal land reclamations are targeted areas of concern because of possible long term ground settlement. In view of the lack of available records and the problem of applying records when available to sites where the soil conditions and the construction methods differ, large scale monitoring work is needed urgently to provide warning on apparent relative sea-level changes. It is based on these findings that subsidence problems may be recognised and addressed using measures including sea defence by dykes and the installation of flood pumping stations.

Acknowledgements

This study would not have been possible without the provision of relevant information by governmental & non-governmental organizations including the Royal Observatory, the Civil Engineering Department, the Drainage Services Department, the Territories Development Department and the Mass Transit Railway Corporation. I am particularly grateful to I.J. Ayson, M.L. Chalmers, S.P. Leatherman, R. Nicholls, H.B. Phillipson, K.H. Tam, R. Wardlaw and D.R. Workman for their assistance. The Croucher Foundation, The University of Hong Kong and the Hui Oi Chow Trust awarded research grants to support this study. Figure 2 is reproduced by courtesy of the Director of Buildings and Lands and Crown copyright is reserved. This paper was a contribution to the Commission on Quaternary Shorelines of the International Union of Quaternary Research.

References

HUANG, J., 1984: Changes in the deltas of the major rivers of China in historical periods. *in* R.O. Whyte (Ed.), *The Evolution of the East Asian Environment Vol. 1 Geology and Palaeoclimatology*, Centre of Asian Studies, The University of Hong Kong, Hong Kong, 320-328.

KWOK, K.W.K., 1990: *Greenhouse effect - allowance in design*. Works Branch Tech. Circ. 6/90, Government Secretariat, Hong Kong, 2pp.

MEACHAM, W. and W.W.S. YIM, 1983: Coastal sand bar deposits at Pui O. *in*, W.W.S. Yim and A.D. Burnett (Eds.), *Geology of Surficial Deposits in Hong Kong*, Abst. 1, Geol. Soc. of Hong Kong and Dept. of Geography & Geology, The University of Hong Kong, Hong Kong, 44-47.

PEART, M.R. and W.W.S. YIM, 1992: Flood hazard in the coastal land reclamations of Hong Kong. *Proc. 2nd U.S.-Asia Conf. Engineering for Mitigating Natural Hazards Damage, June 22-26, 1992, Yogyakarta, Indonesia*, F14/1-14/8.

TAYLOR, B. and D.E. HAYES, 1980: The tectonic evolution of the South China Sea Basin. *in* D.E. Hayes (Ed.), *The Tectonic and Geologic Evolution of Southeast Asian Seas and Islands*, Geophys. Mono. 23, Amer. Geophys. Union, Washington, D.C., 89-104.

YIM, W.W.S., 1991a. An analysis of tide gauge and storm surge data in Kong. *HKMetS. Bull.*, 1(1), 16-23.

YIM, W.W.S., 1991b. Relative sea-level change and long term ground settlement in coastal land reclamations - their assessment and future monitoring. *in* P. Blacker (Ed.), *Reclamation - Important Current Issues*, Hong Kong Inst. Engrs., Hong Kong, 139-151.

YIM, W.W.S., 1991c. Coastal engineering and Quaternary research in Hong Kong. *in* Proc. Inter. Workshop Technology for Hong Kong's Infrastructure Development, Hong Kong University of Science & Technology, Hong Kong, 559-575.

YIM, W.W.S., 1991d. Tide gauge records and crustal stability in the vicinity of the Pearl River mouth, Abstract 7, Inter. Conf. Seismicity in Eastern Asia, October 23-26, 1991, Geol. Soc. of Hong Kong, Hong Kong, 52-53.

YIM, W.W.S. 1992. Future sea-level rise and coastal land reclamation for urbanization in Hong Kong, *HKMetS. Bull.*, 2(2), 3-11.

YIM, W.W.S. 1993. Future sea-level rise in Hong Kong and possible environmental effects. *in* R.A. Warrick, E.M. Barrow and T.M.L. Wigley (Eds.), Climate and Sea Level Change - Observations, Projections and Implications, Cambridge University Press, Cambridge, 349-376.

Mickey Man-Kui Wai

Department of Meteorology

The Florida State University, Tallahassee, FL

Diurnal Atmospheric Secondary Circulations over Hong Kong

ABSTRACT

The secondary circulations found at the Royal Observatory and Waglan Island are primarily generated by the sea-land surface temperature difference. The secondary circulation behaves like a sea-land breeze. A strong signal of topographically forced diurnal secondary circulation in the morning hours during summer months and in the late afternoon during the winter months is found over the Royal Observatory. The secondary flow is strongest during the winter months, but still evident in the summer in some areas. A sharp distinction exists between the annual mean diurnal wind speed between the Royal Observatory and Waglan Island. The effect of urban development on the surface wind surrounding the Royal Observatory is evidently shown by its smaller magnitude when compared to those at Waglan Island. The difference in the magnitude and behavior of the wind speed can be explained in terms of stability, surface roughness, and surface fluxes in the urban part of the secondary circulation and the imbalance between the solar and longwave radiative heating in the marine environment at the other end of the circulation system.

1. Motivation

When the surface wind moves across the warmer Gulf Stream from the adjacent cold water, an increase in the surface wind and changes in the wind direction are found (Sweet *et al.*, 1981). Associated with these changes in the surface wind velocity is a secondary circulation having the descending motion over the cold water and ascending motion over the warm water (Wai and Stage, 1989). In the vicinity of the oceanic front, this secondary circulation influences the local weather. For instance, fog and haze with poor visibility are typical conditions over the cold water. In the warm region, convective phenomena with improved surface visibility are common features. The secondary circulations are also found when warm airstreams are advected across cold ocean eddies (Wai, 1988).

Over land surface, the surface parameters that control the surface and the secondary flows include additional factors such as the geometry of the heated surface area, availability of surface moisture, surface roughness, and terrain effects. The physical features of Hong Kong are complex in both elevation and coastline shape so that nearly all of the above parameters are important.

Besides the Hong Kong mainland (Kowloon Peninsula and the New Territories), the Hong Kong archipelago consists of 236 islands (Figure 1). About 75% of Hong Kong's topography is of a hilly nature. On Hong Kong Island, a main east-west line of ridges begins with Mount Parker at 531 m and ends with Victoria Peak at 552 m. Shallower ridges in the southern part of the Hong Kong Island are oriented in the north-south direction. Similarly, Hong Kong mainland is marked by three chains of ridges running in the northeast to southwest direction. In southwestern part of the Hong Kong mainland, the first ridge begins with Ma On Shan at 702 m and it branches out into Kowloon Peak at 602 m to the south and Lion Rock at 495 m to the west. The second chain includes Tai Mo Shan at 957 m, the highest peak in Hong Kong. The northern and north-western areas are characterized by plains, valleys and smaller ridges with peaks below 650 m. With such a complex terrain, the importance of understanding and predicting the surface and secondary flows cannot be overstated. After all, the boundary layer circulations over the inhomogeneous surface determine the boundary layer transport of pollutants, and thus the level of potential health hazards from airborne materials. To monitor the atmospheric flows over a complex terrain such as Hong Kong, one requires detailed data from a dense observational network

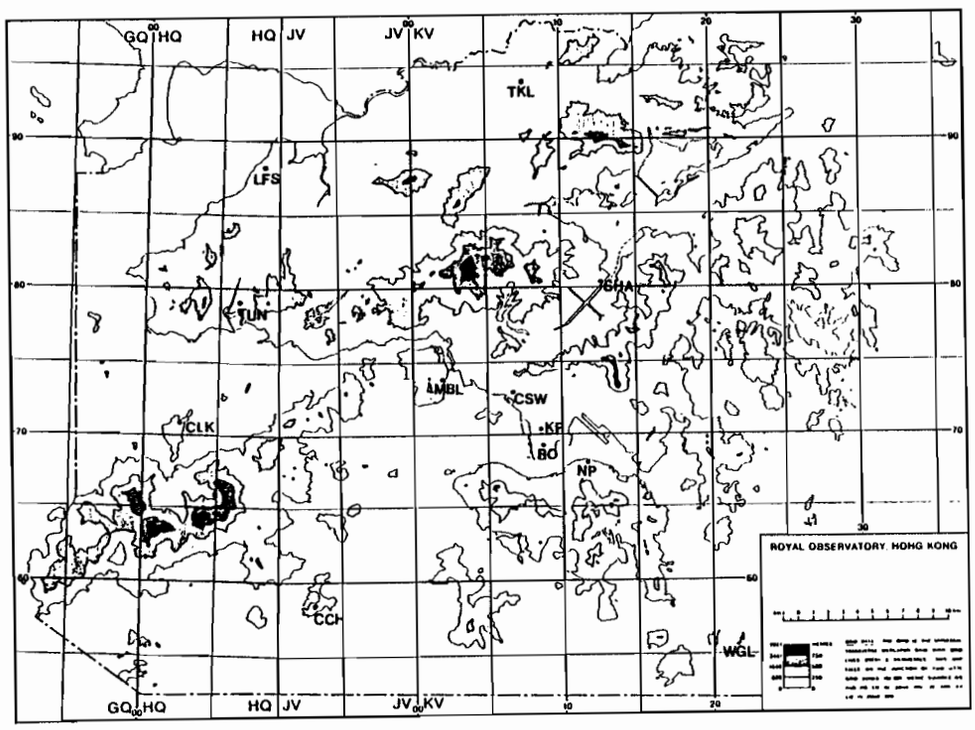

Figure 1 A Topographic Map of Hong Kong.

that covers the entire area. However, this is prohibitively expensive. Thus it is necessary to study the atmospheric flows in detail from a few selected representative sites and then apply what we learn to a model which is capable of generating such flows in order to predict pollutant transport and concentrations. This way, we can improve our skill in the surface wind forecast using the insights provided by both the numerical model and the existing data.

The goal of this paper is to present the analysis of the surface wind records obtained from the Royal Observatory (RO) and Waglan Island (WGL) to learn more about the mechanisms governing the diurnal behavior of the secondary flows.

2. Data

A complete record of 1988 hourly wind velocity observations at the Royal Observatory and Waglan Island is used to compute the mean and secondary atmospheric flows. The observations of surface temperature at the Royal Observatory and the sea surface temperature (SST) taken at the North Point Fire Station (NP) and Waglan Island are also used to augment the discussion of the secondary flows.

Waglan Island, a tiny remote island surrounded mostly by open sea, is located in the south eastern corner of Hong Kong. The elevation of Waglan Island is less than 50 m. Waglan Island is uninhabited, but serves as a site for weather instrument platforms, providing vital weather elements to ships entering Hong Kong harbor. In contrast to the marine environment at Waglan Island, the Royal Observatory, located near the tip of the Kowloon Peninsula, is surrounded by well-developed urbanization including both commercial and residential buildings.

3. Computation of secondary wind velocity

Three averaging methods are used to obtained the secondary flows: (1) time averaging, (2) ensemble averaging, and (3) Reynolds averaging. Each method is outlined briefly as below.

a. Time averaging

The time average applies at one specific point in space over time period T.

$$\overline{u}(t,s,n) = \frac{1}{T}\sum_{t=0}^{T-1} u(t,s,n) \qquad 3.1$$

where $u(t,s,n)$, a scalar variable, is a function of time (t), space (s), and number of repeated observations or experiments (n).

b. Ensemble averaging

The ensemble average is summed over n repeated observations or experiments at one specific point and at a specific time.

$$\overline{u}(t,s,n) = \frac{1}{N}\sum_{n=0}^{N-1} u(t,s,n) \qquad 3.2$$

c. Reynolds averaging

The instantaneous scalar variable is decomposed into three components:

$$u(t,s,n) = u(t,s,n)_l + u(t,s,n)_s + u(t,s,n)_m \qquad 3.3$$

where $u(t,s,n)_l$ is the large-scale variation, $u(t,s,n)_s$ is the secondary-scale variation, and $u(t,s,n)_m$ is the microscale variation which includes a turbulence part and instrument errors. When we apply the averaging methods, $u(t,s,n)_m$ will approach zero.

To reduce the hourly observations to the secondary flows, let us define the daily running mean wind ($[\overline{u}]_t$, $[\overline{v}]_t$) and the secondary surface wind (u_t', v_t') as follows:

$$[\overline{u}]_t = \frac{1}{T}\sum_{t-12}^{t+12} u(t,s,n) \qquad 6.4a$$

$$[\overline{v}]_t = \frac{1}{T}\sum_{t-12}^{t+12} v(t,s,n) \qquad 6.4b$$

$$u_t' = u_t - [\overline{u}]_t \qquad 6.5a$$

$$v_t' = v_t - [\overline{v}]_t \qquad 6.5b$$

Here T is the time period in hours, ($[\overline{u}]_t$, $[\overline{v}]_t$), and (u_t',v_t') are in m s^{-1}. Note that the running daily mean wind speed is used for the complete wind record because it preserves a smooth transition of the diurnal wind cycle even during the passage of the nocturnal atmospheric surface fronts which would strongly affect a smaller subset of the data if the daily mean were calculated from midnight to midnight. The zonal and meridional components of the secondary wind speed are ensemble averaged for each month. The use of Equations 6.4 and 6.5 is to remove the transient signals resulting from the varying synoptic and mesoscale-scale conditions in order to isolate the diurnally forced local circulation. For comparative purposes, the mean diurnal wind cycle is also calculated by ensemble averaging the hourly observations of the zonal and meridional components for each month.

A time sequence of the mean and secondary wind vectors at the Royal Observatory and Waglan Island is calculated to illustrate the complete annual cycle of the atmospheric surface flows. A comparison of the mean and secondary flows between these two sites not only gives the temporal and spatial variation in the flows but also indicates their underlying differential surface forcing.

4. Annual cycle of the mean surface flows

The monthly diurnal variations of the wind velocity at the Royal Observatory and Waglan Island are shown in Figures 2 and 3. Reviewing the pattern of the changes in the surface wind velocity, several interesting features are found. In spite of the fact of being separated by Hong Kong Island which has several peaks over 500 m, both sites show remarkably similar surface atmospheric circulations.

a. Royal Observatory

The winter easterly wind persists from January through April and dominates the flow (Figure 2). The easterly surface wind shifts to southeasterly in May and then veers to more southerly in June. Throughout summer months, the surface wind maintains southerly or southwesterly flows. In September, the surface wind begins to shift back to northeasterly, except for a few hours in the afternoon. In the last three months of the year, easterly or east northeasterly winds prevail. There is little diurnal wind reversal shown in the mean winds. The effect of urban development on the surface wind surrounding the Royal Observatory is shown by the small magnitude of the mean surface wind speed. The increased surface roughness elements produce a larger

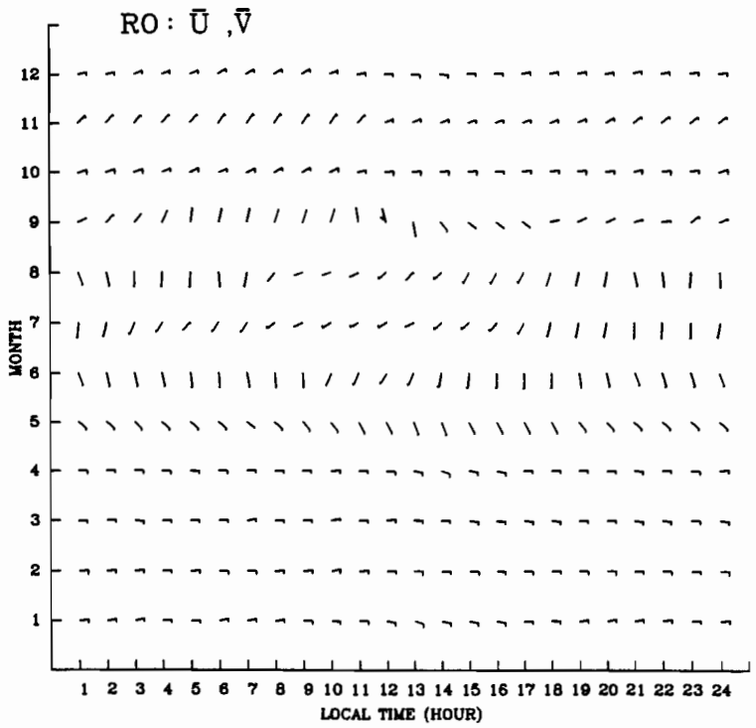

Figure 2 Annual cycle of mean diurnal wind velocity at the Royal Observatory. Each full bar represents a wind speed of 10 ms^{-1}.

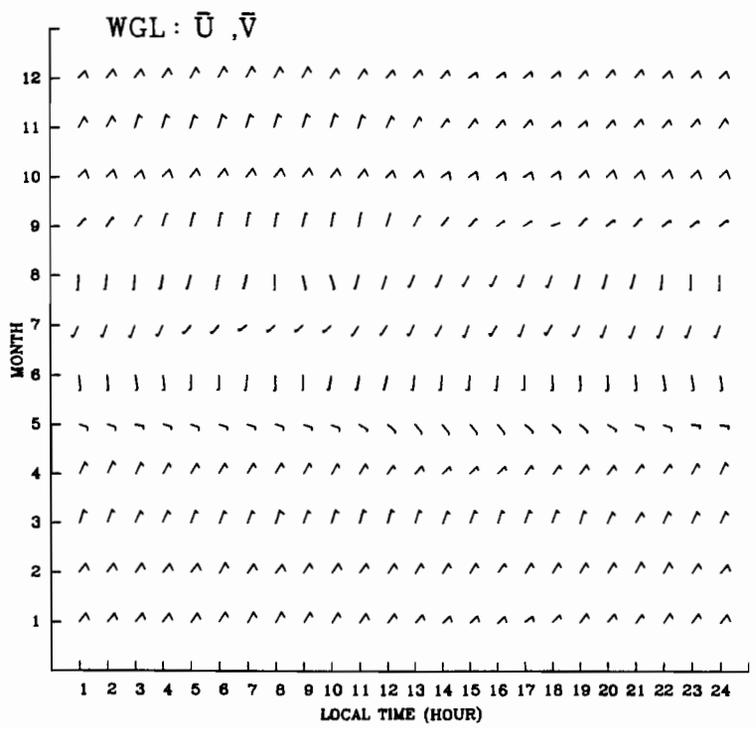

Figure 3 Annual cycle of mean diurnal wind velocity at the Waglan Island. Each full bar represents a wind speed of 10 ms^{-1}.

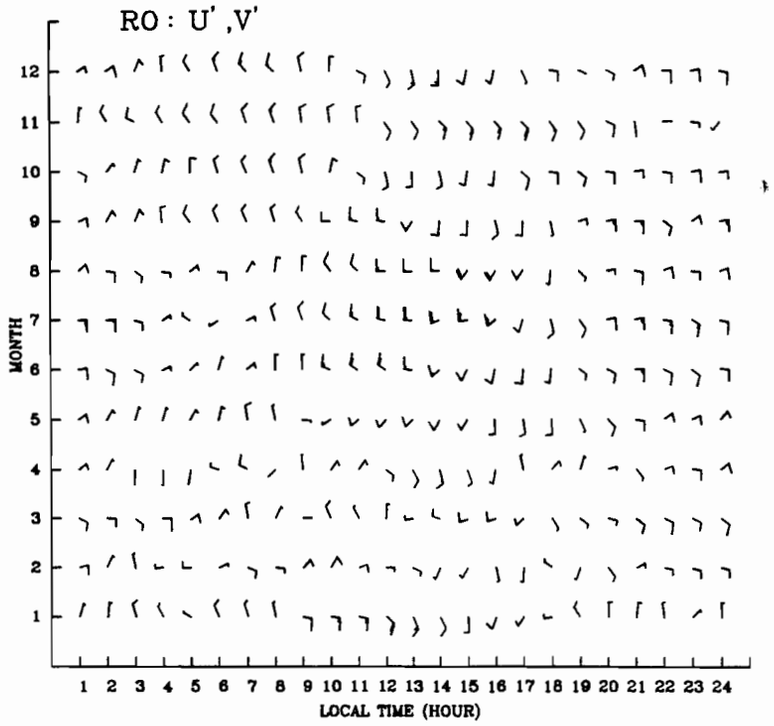

Figure 4 Annual cycle of diurnal secondary wind velocity at the Royal Observatory. Each full bar represents a wind speed of 0.2 ms^{-1}.

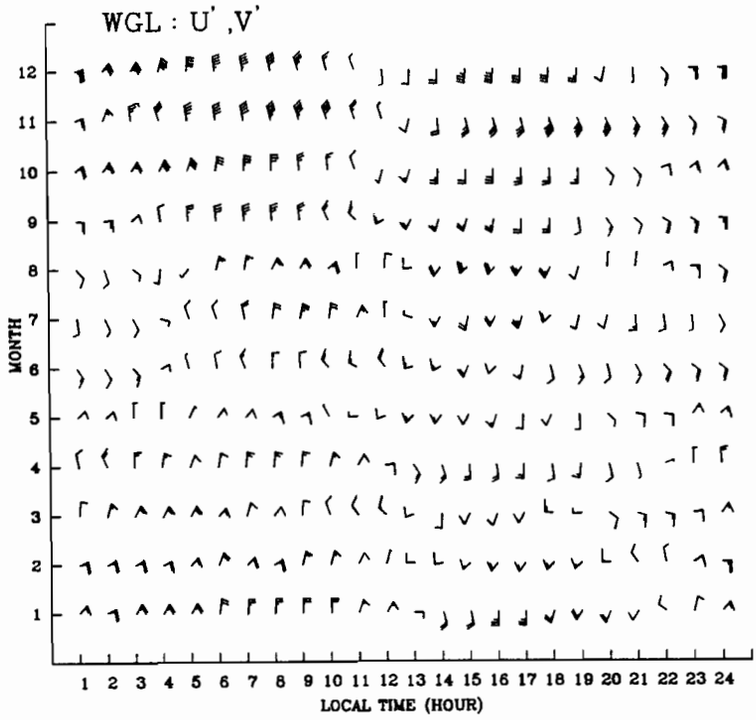

Figure 5 Annual cycle of diurnal secondary wind velocity at the Waglan Island. Each full bar represents a wind speed of 0.5 ms^{-1}.

surface friction and evidently lead to reduction of the surface wind speed. A detailed discussion will be given in Section 6.

b. Waglan Island

The winds observed at this site closely follow those above. Northeasterly wind prevails at Waglan Island from January to April (Figure 3). The northeasterly wind shifts to east-south-easterly or southeasterly in May, and the surface wind remains southerly or southwesterly throughout summer months. In September, it changes to northeasterly and prevails for the last three months of the year. Little diurnal change is found in the mean wind direction.

The annual cycle of the mean surface wind shown in Figures 2 and 3 agrees with the regional atmospheric flows described by Domros and Peng (1988). During the winter months, a strong surface anticyclone develops over mid-Siberia and Mongolia while the Aleutian Low forms in the Pacific northwest. These two systems give an easterly component to the surface wind along the Southern China coast, including the Hong Kong area. Beginning in March, the intense winter anticyclone and cyclone weaken, and by April the pressure gradient has weakened over most parts of China. By May, a low pressure system develops over Northwestern India and Pakistan subcontinent. Over the Pacific, the northern low pressure system changes to a semi-permanent central Pacific high pressure system. This pair of surface pressure systems persists throughout the summer months. Thus, the surface wind along the South China has a very strong southerly component. In September, the thermal cyclone over India and Pakistan weakens and a continental anticyclone is already weakly formed over Mongolia. The surface wind along the South China shifts back to a strong easterly component during the winter months.

5. Evidence of secondary flows

The secondary flows at the Royal Observatory and Waglan Island are described in this section. The discussion on the linkage of the surface forcing and the secondary circulations is also presented.

a. Royal Observatory

The secondary circulation winds at the Royal Observatory are weaker and more variable in direction (Figure 4). The secondary flow is evident in the diurnal shift of the wind direction. However, the periodicity and onset of wind reversals are irregular. For instance, a sharp wind shift from northwesterly to southeasterly occurs between 0800 and 0900 in both January and May. Between February and April, the surface wind is more highly variable. This is correlated with decreased forcing due to relatively weaker land-sea surface temperature differences. Between October and December, the wind shift occurs between 1100 and 1200 hours. In all cases when it occurs, the southeasterly changes back to northerly around 1800 hours. During summer months, the secondary wind direction backs gradually till 1800 to 2000 hours indicating the stronger relatively influence of the secondary flow.

b. Waglan Island

The secondary wind velocity at Waglan Island (Figure 5) shows a much clearer and more regular periodicity in the diurnal wind shift throughout the year. A sharp wind shift from northwesterly to southerly occurs between 1100 and 1300 hours. After the reversal, the surface wind remains southerly until 2100 or 2200 hours at which it rotates back to northerly. The diurnal wind system behaves like a classic sea-land breeze circulation. During summer months of June and July, the onshore flow lasts until 0300 hours before the offshore flow returns.

c. Linkage of surface forcing and secondary flows

Further evidence of the linkage of surface forcing and the secondary circulation is presented here by correlating the morning and evening observations of sea-land surface temperature. For this purpose, the observations of SST at 0700 and 1400 hours at the North Point Fire Station and 1700 hours at Waglan Island are selected. Correspondingly the observations of surface temperature at 0700 and 1700 hours at the Royal Observatory are chosen. Figure 6 displays profiles of the monthly surface temperature and secondary wind velocity.

The top panel in Figure 6a shows the surface temperature at the Royal Observatory (solid lines) and SST at the North Point Fire Station (dashed lines) at 0700 hours. The monthly SST is warmer than the land surface temperature during winter months (October to February) by 1 to 3 degrees while the land surface temperature is larger than the SST by less than 1 degree from April to August. Thus, during winter months, offshore flows prevail. The secondary circulation system acts like a land breeze or a down-slope wind, or both. During the summer months, the surface secondary wind is still an offshore flow

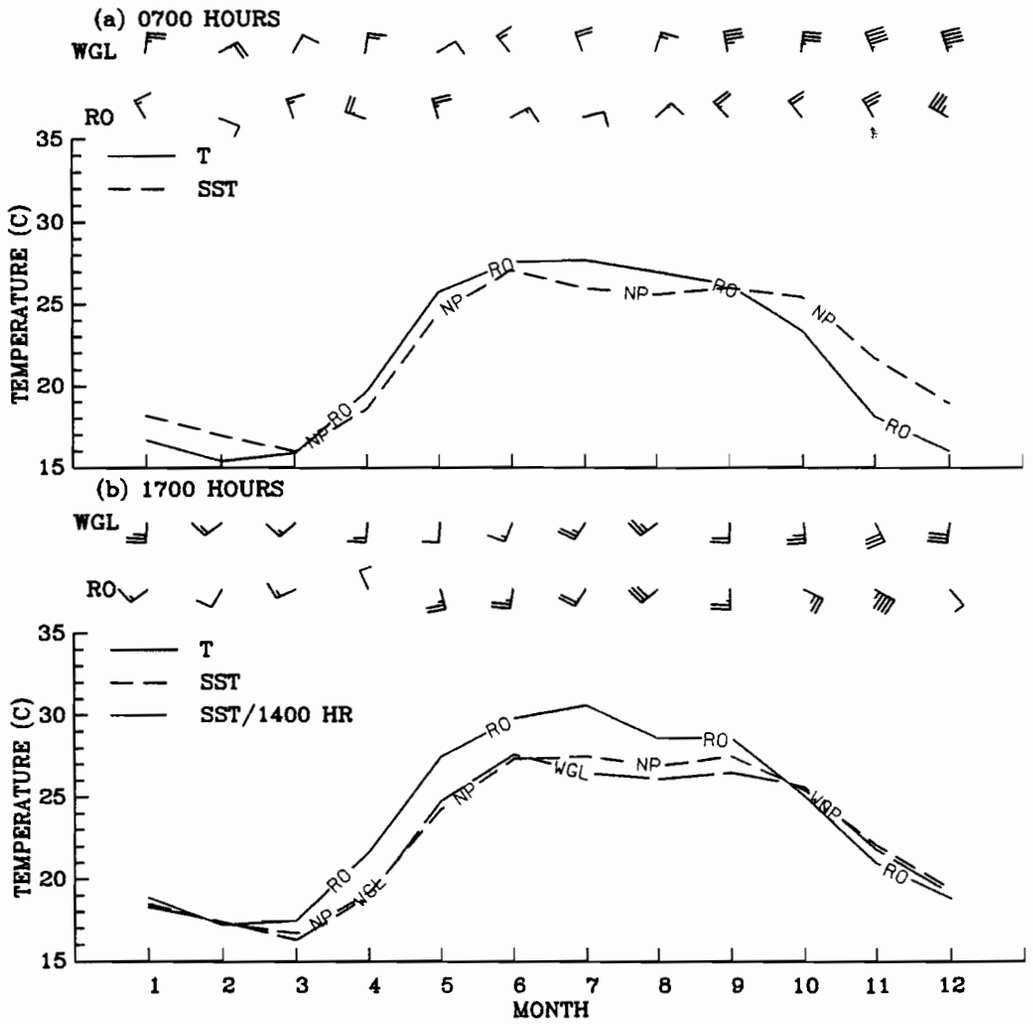

Figure 6 Profiles of monthly mean surface temperature (solid line), sea surface temperature (dashed lines), and secondary wind velocity in (a) the morning and (b) afternoon hours. Each full bar represents a wind speed of 0.5 ms^{-1} at Waglan Island (WGL) and 0.2 ms^{-1} at the Royal Observatory (RO). North Point Fire Station is represented by the symbol NP.

even though the SST is slightly cooler than the surface temperature at the Royal Observatory. The heat island effect surrounding the Royal Observatory as a result of urbanization limits the nocturnal cooling (slower rate) as compared to elsewhere, which should maintain a relatively higher surface temperature and induce an onshore flow. Thus, the presence of offshore flow during the morning hours indicates that the topographic effect (downslope flow) on the surface secondary wind at the Royal Observatory site is the primary forcing. The secondary surface wind at Waglan Island responds to a larger scale of land-sea surface temperature differences.

The bottom panel in Figure 6b shows the monthly surface temperature at the Royal Observatory at 1700 hour and the SST at the North Point Fire Station (short dashed line) at 1400 hours and at Waglan Island (long dashed lines) at 1700 hours. As the land surface temperature rises during the day, the sea-land temperature difference becomes smaller in January and February. Between October and December, the land surface temperature is cooler than the SST on the order of 1 degree. From March onwards, the land surface temperature is warmer than the SST by about 1 degree and increases to about 3 degrees in July. As the maximum solar insolation has passed in July, the land surface temperature is

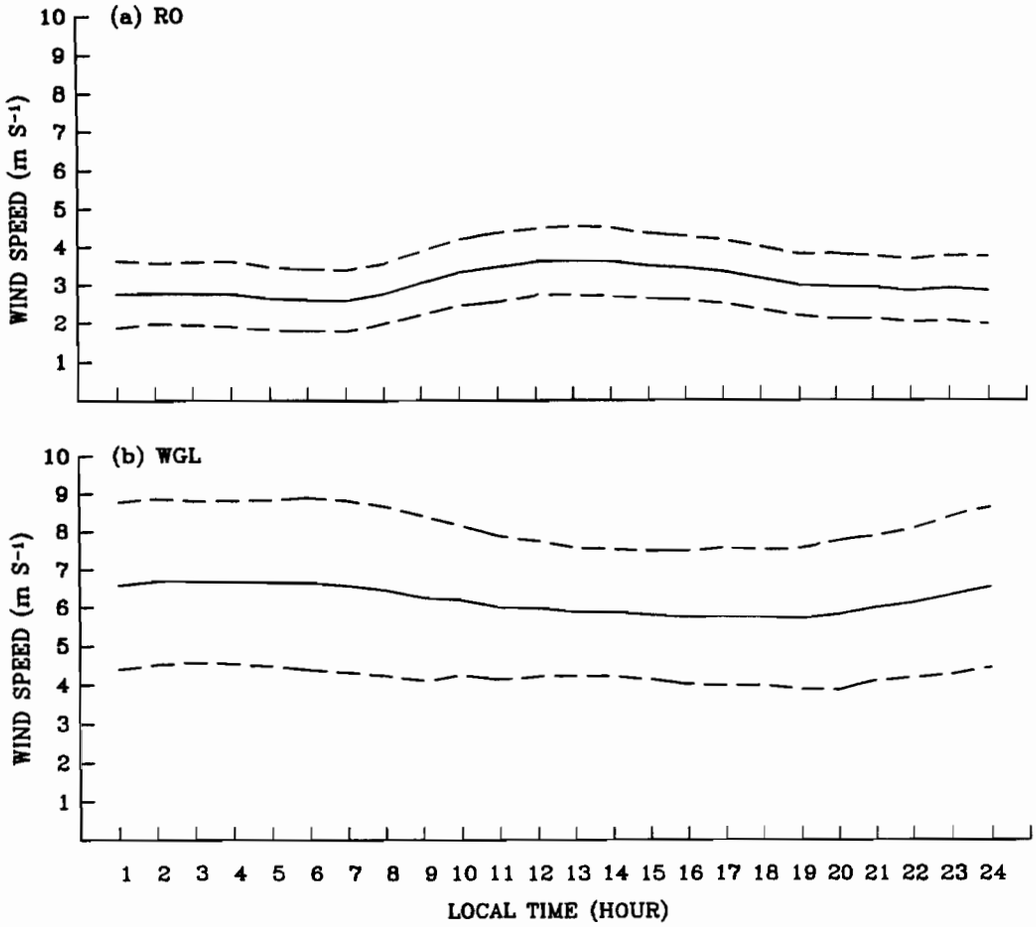

Figure 7 Annual mean diurnal wind speed at (a) the Royal Observatory and (b) Waglan Island. The dashed lines indicate plus and minus one standard deviation from the mean.

still warmer but by a smaller differential becoming less than 1 degree in September. The SST difference between the North Point Fire Station and Waglan Island is very small. The monthly secondary wind velocities at 1700 hours are displayed above the SST profiles. The surface wind at both sites are dominated by the southerly component. Relatively strong south-westerly secondary wind persists throughout summer months (June through August). The strong southerly component of the secondary surface wind correlates well with sea-land surface temperature difference. When the land-surface temperature difference is minimal (October through February), no dominant wind direction is found at either site. Under this surface temperature condition, the topographic effect on the surface secondary wind will play the most important role in maintaining the onshore secondary flow at the Royal Observatory. The secondary wind is dominated by upslope-downslope flow. At Waglan Island, the southerly flows is in response to larger scale land-surface temperature differences.

6. Controlling mechanism for diurnal wind speed

The mean and secondary surface wind at the Royal Observatory in Figure 2 show that the surface winds are weaker than those at Waglan Island. To examine the physics governing the diurnal behavior of the wind at both sites, the annual mean diurnal surface wind is shown Figure 7. The dash lines indicate plus and minus one standard deviation. A small standard deviation at the Royal Observatory indicates that the variability in the annual diurnal surface wind is consistently small. These two profiles show sharp difference in the characteristics of the urban and marine environment. At the Royal Observatory, the wind speed drops from 3.6 m s^{-1} near 1400 hours, the time of maximum heating, to 3 m s^{-1} near 1900 hours. The wind speed gradually decreases throughout the evening and the early morning hours until 0600 hours at which the wind speed reaches its minimum of 2.6 m s^{-1}.

Shortly after sunrise, the wind speed begins increasing rapidly, reaching a maximum in the late afternoon. Such a pattern of the diurnal behavior in the wind speed is similar to previous observations in the Minnesota Experiment (Caughey *et al.*, 1979), the Wangara Experiment (Mahrt, 1981), and the First ISLSCP Field Experiment (FIFE) (Smith *et al.*, 1993). The reduction in the magnitude of surface wind speed during the evening transition period in the previous experiments ranges from 1.5 m s^{-1} to 2 m s^{-1}. The small drop in the wind speed (less than 1 m s^{-1}) during the evening transition period at the Royal Observatory is probably due to the heat island effect, which prevents the lower boundary layer from becoming stratified rapidly.

The marine diurnal cycle of the wind speed at Waglan Island is nearly opposite to the diurnal cycle at the Royal Observatory. After sunset, the wind speed gradually increases to 6.5 m s^{-1} throughout the evening and the earlier morning hours to 7 m s^{-1} near 0600 hours. When sunrise begins, the wind speed begins to drop and reaches its minimum speed in the late afternoon. Such a behavior in the diurnal change in the wind speed can be explained in terms of solar heating and longwave radiative cooling near the surface. During the night, the air parcels over the sea surface are cooled by longwave radiation while the SST changes little or even remains steady. The air has its lowest temperature in the early morning hours, giving the largest sea-air temperature difference. The surface layer tends to be less stratified and may even become unstable, leading to increased surface heat fluxes. By late afternoon, the solar heating will overcome the longwave cooling effect, and the differential heating will produce a smaller sea-air temperature and lead to small or even negative heat fluxes. Thus the surface layer will become stratified. A similar pattern of diurnal wind speed to that observed at Waglan Island is also found in a numerical study of the break up of marine boundary layer clouds (Wai, 1991a,b).

The diurnal behavior of the annual mean wind velocity at the Royal Observatory and Waglan Island can be explained in terms of the effects of land-sea breeze, terrain, urbanization, seasonal and diurnal changes. Considering the forcing mechanisms that lead to diurnal changes in the wind speed, only the variation of the surface sensible heat flux and surface terrain can generate changes consistent with those observed. The observed effects of land-sea breeze, urbanization, seasonal and diurnal changes are all consistent with variation of the surface sensible heat fluxes.

To obtain insight into what physical mechanism could govern the differential diurnal variation in the surface wind, we can relate the friction velocity (u_*) to the surface heat fluxes. If u and v components are expressed as

$$u = -S\cos\theta \qquad 6.1a$$

$$v = -S\sin\theta \qquad 6.1b$$

where S is the wind speed, and θ is the wind direction. The wind speed and direction can be expressed as:

$$S = (u^2 + v^2)^{\frac{1}{2}} \qquad 6.1c$$

$$S = u_* \left[\ln\left(\frac{z}{z_o}\right) + \frac{f_1}{k} \right] \qquad 6.2$$

$$\sin\theta = -\frac{v}{S} \qquad 6.3$$

z_o is the surface roughness length, f_1 the similarity function, k von Karman's constant. Furthermore if the surface heat flux is approximated by

$$\overline{w't'} = K\frac{\partial \overline{T}}{\partial z} \qquad 6.4$$

where W' is the perturbation vertical velocity, t' is the perturbation surface air temperature, and the thermal eddy diffusivity (K) is proportional to the turbulent length scale (l) and u_*; then when the effect of surface stratification is small, l is proportional to z and the surface heat flux can be expressed as

$$\overline{w't'} = u_* z\frac{\partial \overline{T}}{\partial z} \qquad 6.5$$

When the surface layer temperature gradually becomes stably stratified, the eddy motion is suppressed by the stability. As the surface layer

asymptotically approaches 'z-less' (height independent) stratification (Wyngaard, 1973), the eddy size is given by the stability length (L). Thus, l is proportional to L, which is given by:

$$z \propto L = u_* (gT_o^{-1} \frac{\partial \overline{T}}{\partial z})^{-\frac{1}{2}} \qquad 6.6$$

where T_o is the basic state temperature. Therefore, after substituting z (equation 6.6) into equation 6.5 and rearranging, we can express

$$u_*^2 = \overline{w't'} (gT_o^{-1})^{\frac{1}{2}} (\frac{\partial \overline{T}}{\partial z})^{-\frac{1}{2}} \qquad 6.7$$

for the stable surface layer. On the other hand, u_* during the daytime is directly proportional to the cubic root of surface heat flux and the depth of the boundary layer height (h) for free convection *i.e.*

$$u_* = w_* = [(gT_o^{-1})\, h\, \overline{w't'}]^{\frac{1}{3}} \qquad 6.8$$

From equation 6.6, we see that u_* decreases with increased surface stratification in the stable boundary layer. Also the magnitude of u_* is directly proportional to the surface heat flux as given in equations 6.7 and 6.8. From equation 6.2, two mechanisms lead to the reduction of the wind speed. First, the surface wind would be expected to drop rapidly with the decay of u_* (the decrease of surface sensible heat flux and increased surface stratification). Second, the wind speed would also decrease with the increase in the surface roughness element length. For example, the values of z_o increase by an order of magnitude, from 10^{-4} m for the calm open ocean to 10^{-3} m over coastal areas. Over land, the values of z_o increase by an order of magnitude in the following types of landscapes: 10^{-2} m over the fairly level grass plains; 10^{-1} m over farmlands; 1 m over the center of small town; and several meters over the center cities with skyscrapers (Smedman-Hogstrom and Hogstrom, 1978). Thus, given the same values of z, u_*, and f_l, the wind speed will decrease over the landscapes in the following order : (1) open ocean; (2) coastal water; (3) fairly level grass plains; (4) farmland; (5) center of large towns; and (6) center of cities with skyscrapers. Therefore, the diurnal wind speed at the Royal Observatory is expected to be consistently smaller than those at Waglan Island.

The terrain effect needs to be considered in the Hong Kong domain because of the hilly nature. To assess its impact, consider a scale analysis within the u-component of the momentum equation:

$$\frac{\partial u}{\partial t} + \underline{v} \cdot \nabla u - f(v - v_g) - (g\frac{T'}{T_o}) \sin\alpha + \frac{\partial \overline{u'w'}}{\partial z} = 0 \qquad 6.9$$

Here the second term is the advection term expressed in its vector form, the third term is the Coriolis departure (ageostrophic) term, the fourth term is the buoyancy term (which also represents downslope drainage acceleration), and the last term is the wind stress divergence term. The slope factor in the buoyancy term is the terrain slope. To simplify the discussion, let us assume that the initial flow is horizontally homogeneous with zero mean vertical motion. Thus, equation 6.9 can be reduced to

$$\frac{\partial u}{\partial t} - f(v - v_g) - (g\frac{T'}{T_o}) \sin\alpha + \frac{\partial \overline{u'w'}}{\partial z} = 0 \qquad 6.10$$

If we approximate the stress divergence term by $u_*^2 h^{-1}$, and take $f = 10^{-4}$ s^{-1}, v-v_g = 5 m s^{-1}, h = 100 m, u_* = 0.1 m s^{-1}, $g \doteq 9.8$ m s^{-2}, T_o = 300 K, T' = 3 K, and assume a slope of 1 part in 1000, we obtain scales for the Coriolis departure term, the terrain effect term, and stress divergence terms of 10^{-4} s^{-2}. This demonstrates for a slope of 1:1000 that the terrain term is of the same order as the friction term. In the Kowloon Peninsula area, the slope is about 60 parts in 1000. Thus, the terrain effect can produce drainage flows which are dominant even in the presence of contrasting land-sea surface temperature differences. The full details on how the terrain modifies the surface flow over a complex terrain requires a complete dynamic framework and realistic surface conditions with scaled topography in order to understand and predict complex local surface forcing and secondary flows.

7. Conclusions

The secondary circulations found at the Royal Observatory and Waglan Island are primarily generated by the sea-land surface temperature differences. The secondary circulation behaves like sea-land breeze. A strong signal of topographically forced diurnal secondary circulation in the morning hours during summer months and in the late afternoon during the winter months is indicated by the secondary flows over the Royal Observatory. The chain of ridges north of the Kowloon Peninsula is probably important in sustaining the secondary surface wind in these two cases. The secondary flow is strongest during the winter months, but still evident in the summer in some areas. A sharp distinction exists between the annual mean diurnal wind speed at the Royal Observatory and Waglan Island. The effect of urban development on the surface wind surrounding the Royal Observatory is shown by its smaller magnitude when compared to those at Waglan Island. The difference in the magnitude and behavior of the wind speed can be explained in terms of stability, surface roughness, and surface sensible heat fluxes in the urban part of the secondary circulation and the imbalance between the solar and longwave radiative heating in the marine environment at the other end of the circulation system. Thus the annual cycle of the observed diurnal wind structure over the region gives us some clues to the nature of relative dominance of the complex local forcing in the Hong Kong area.

Acknowledgements

The author wishes to thank retired US Navy Lieutenant Commander Patrick Welsh for his discussion towards the improvement of this paper. The meticulous and critical comments received from three anonymous reviewers are appreciated. A data tape, a handbook of surface observations in Hong Kong 1988, and the topographic maps of Hong Kong provided by the Royal Observatory to the author are gratefully acknowledged.

References

CAUGHEY, S.J., J.C. WYNGAARD and J.C. KAIMAL, 1979: Turbulence in the evolving stable boundary layer. *J. Atmos. Sci.*, **36**, 1041-1052.

DOMROS, M. and G. PENG, 1988: *The Climate of China*, Springer-Verlag, Berlin, 360 p.

MAHRT, L., 1981: The early evening boundary layer transition. *Quart. J. Roy. Meteor. Soc.*, **107**, 329-343.

SWEET, W., R. FETT, J. KERLING and P. LaVIOLETTE, 1918: Air-sea interaction effects in the lower troposphere across the north wall of the Gulf Stream. *Mon. Wea. Rev.*, **109**, 1042-1942.

SMEDMAN-HOGSTROM, A.-S., and U. HOGSTROM, 1978: A practical method for determining wind frequency distributions for the lowest 200 m from routine meteorological data. *J. Applied Meteor.* **17**, 942-954.

SMITH, E.A., M.M.-K. WAI, H.J. COOPER, M.T. RUBES and A. HSU, 1993: Linking boundary layer circulations and surface processes during FIFE89. Part 1: Observational analysis using FIFE Information System (FIS). Accepted for publication in *J. Atmos. Sci.*

WAI, M.M.-K., 1988: Modeling the effects of spatial sea surface temperature on the marine atmospheric boundary layer. *J. Applied Meteor.*, **40**, 241-267.

WAI, M.M.-K., and S.A. STAGE, 1989: Dynamical analyses of marine atmospheric boundary layer structure near the Gulf Stream oceanic front. *Quart. J. Roy. Meteor. Soc.*, **115**, 29-44.

WAI, M.M.-K., 1991a: The breakup of marine boundary-layer clouds over an inhomogeneous sea surface temperature field. *Boundary-Layer Meteor.*, **57**, 139-165.

WAI, M.M.-K., 1991b: Persistence of marine boundary layer clouds in a case with inhomogeneous surface forcing. *Beitr. Phys. Atmos.*, **64**, 335-338.

WYNGAARD, J.C., 1973: On surface layer turbulence. *in* D.A. Haugen (Ed.), *Workshop on Micrometeorology*. Amer. Meteor. Soc., Boston, 101-149.

C.M. Shun and K.S. Leung

Royal Observatory

Hong Kong

The First Radioactivity and Ozone Soundings in Hong Kong

ABSTRACT

Upper air meteorological measurements in Hong Kong, which started in 1921, reached another milestone in 1993 - a new sounding system known as DigiCORA was installed at the King's Park Meteorological Station of the Royal Observatory in February 1993. Having benefited from technological advance, the DigiCORA system is able to support measurement of vertical radioactivity and ozone profiles using specially designed radiosondes.

The first radioactivity sounding and ozone sounding in Hong Kong were made respectively on 26 February 1993 and 4 March 1993. While the first radioactivity ascent provides information on the vertical distribution of natural background radiation levels, the ozone sounding on 4 March 1993 allows us to have the first glimpse of interesting features of the ozone distribution aloft. The first ozone profile is also briefly compared with one obtained over Okinawa, Japan, at around the same time. Future plans for carrying out radioactivity and ozone soundings in Hong Kong are also described.

Introduction

A new upper-air sounding system known as DigiCORA (Vaisala, 1992) was installed at the King's Park Meteorological Station of the Royal Observatory in February 1993. The DigiCORA system would replace the existing MicroCORA system which has been in operation since January 1981.

Apart from having improved windfinding and better data presentation capabilities, the DigiCORA system supports measurement of vertical radioactivity and ozone profiles using specially designed radiosondes. The first radioactivity sounding and ozone sounding were made respectively on 26 February 1993 and 4 March 1993. These ascents provide us with the very first upper-air radioactivity and ozone data sets for Hong Kong.

Radioactivity Sounding

The sonde used for radioactivity sounding consists of a radioactivity sensor, a special version of the standard radiosonde RS 80-15FR and an interface for connecting the radioactivity sensor to the radiosonde (Vaisala, 1993a). In addition to obtaining conventional PTU (pressure, temperature and humidity) data, the radioactivity sonde also measures vertical profiles of total beta and gamma radiation levels (in counts per second) in the troposphere and lower stratosphere.

The radioactivity sensor (type NSS 13) is shown in Figure 1. It has two Geiger-Muller (G-M) tubes, one measuring only gamma radiation while the other measuring both gamma and high energy (> 0.25 MeV) beta radiation. The G-M tubes measure the ionization of the tube filling gas as a result of interactions between the radiation and tube wall material, giving the radiation levels in number of counts per second (c/s). This count rate is measured once in 0.293 second. Before launch, the NSS 13 radioactivity sensor is connected to the RS 80-15FR radiosonde which measures PTU data. The ready-to-launch package only weighs about 380 g.

The ground equipment consists of the DigiCORA system, an IBM PC compatible computer, and a dot matrix printer (Vaisala, 1993a). A schematic diagram of the complete system for radioactivity sounding is shown in Figure 2.

Vertical profiles of beta and gamma radiation levels, pressure, temperature and humidity can be

Figure 1 Radioactivity sensor NSS 13 showing two Geiger-Muller tubes - gamma tube (right) and beta tube (left).

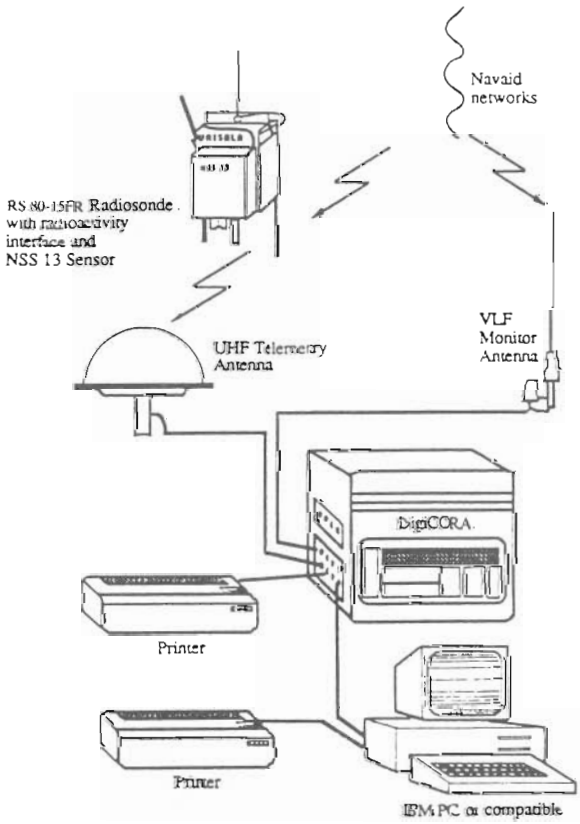

Figure 2 Schematic diagram showing a complete DigiCORA system for radioactivity sounding (Vaisala, 1993a).

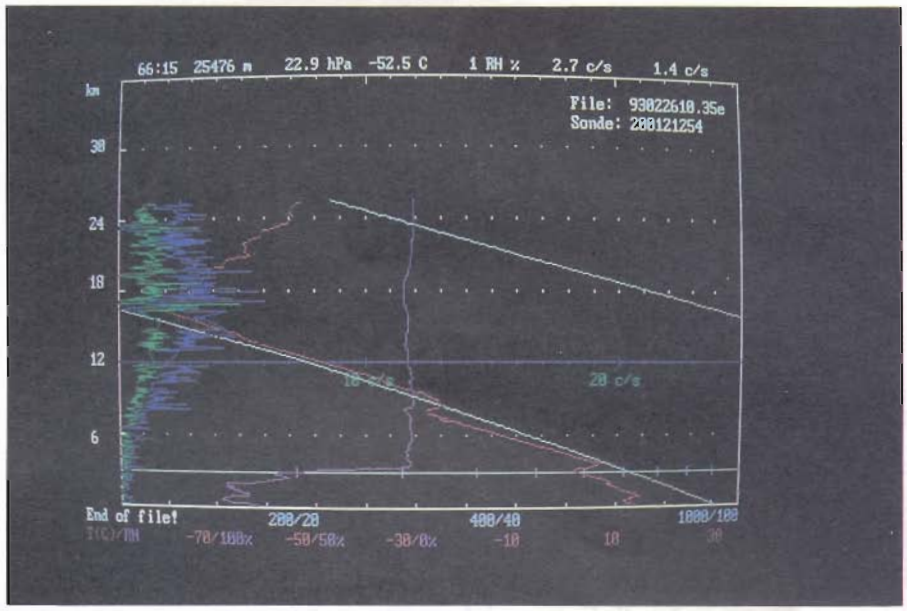

Figure 3 Real-time display of the vertical profiles of beta radiation level (green), gamma radiation level (blue), pressure (white), temperature (red) and humidity (pink) measured at 03 UTC on 26 February 1993.

displayed on the IBM PC compatible computer in real-time using a dedicated software. Those pertaining to the radioactivity ascent at 03 UTC on 26 February 1993 are shown in Figure 3. The balloon burst near 25.5 km (23 hPa). Generally higher radiation levels were detected at high altitudes than at low altitudes. Both the beta and gamma radiation levels attained their maxima of around 5 to 6 counts per second near 17 km (90 hPa). These vertical profiles are consistent with the distribution of natural background radiation which mainly originates from cosmic rays. The maximum layer was believed to be the result of the interaction of two phenomena: the rapid decrease of secondary low energy neutron flux with decreasing altitude, and the vertical distribution of air density (Junge, 1963).

Ozone Sounding

The sonde used for ozone sounding consists of an ECC-type ozone sensor, a special version of the standard radiosonde RS 80-15FE and an interface for connecting the ozone sensor to the radiosonde (Vaisala, 1993b). In addition to obtaining conventional PTU data, the ozonesonde measures the vertical profile of ozone concentration (in mPa) in the troposphere and lower stratosphere.

The ozone sensor (type ECC-5A) is shown in Figure 4. It consists of an electrochemical concentration cell (ECC) and a constant volume pump. The electrochemical reactions between ozone and the electrolytes of the cell give rise to a small electric current proportional to the ozone abundance of the sampled air. The current is measured by an OIF 11 interface board and converted to digital form for transmission to the ground equipment. About five ozone readings are obtained in 1.56 second. Before launch, the radiosonde which measures PTU data is attached to a polystyrene box containing the ozone sensor and interface. The ready-to-launch package weighs about 1050 g. Apart from the dedicated software, the ground equipment is essentially the same as the set-up for radioactivity sounding.

The pre-launch preparation (Vaisala, 1993b) requires a special unit known as an Ozonizer/Test Unit. Using the Ozonizer/Test Unit, ozone in controlled concentrations can be generated for comparing the sensor response against that of a calibrator sensor within the Unit. Supplementary tools such as vacuum/ pressure measurement gauge, air flow meter, ozone destruction filter, thermometer, precise balance, simple laboratory ware and chemicals are also needed during the preparation.

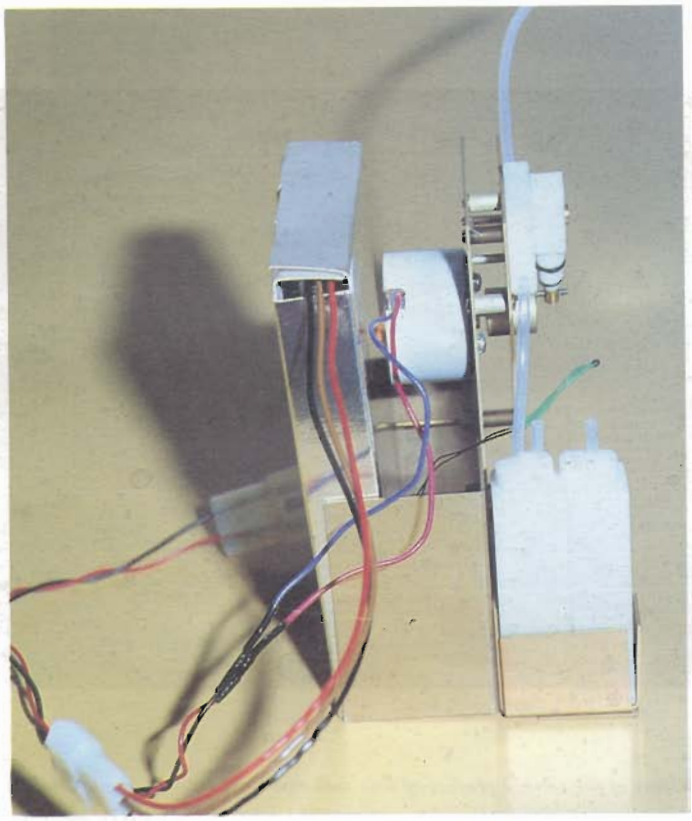

Figure 4 Ozone sensor ECC-5A showing the electrochemical concentration cell (bottom right) and constant volume pump (top right).

The pre-launch preparation takes 3 to 4 hours, and is much more complicated than the preparation of an ordinary radiosonde. To ensure good data quality, the preparation procedures have to be carried out carefully. These procedures include: (a) advance preparations several days prior to release - including preparation of anode and cathode solutions for the sensor, cleaning of equipment, checking of overall performance of the sonde, and charging of the sensor with anode and cathode solutions; (b) preparations on the day of release - including cleaning of equipment and detailed checking of overall performance of the sonde, in particular, the air pump and sensor are subject to various calibration acceptance tests; and (c) preparations right before release - including flight package preparations and measurements of sensor background current and surface pressure.

The real-time display of the vertical profiles of ozone concentration, pressure, temperature and humidity pertaining to the ozone ascent at 03 UTC on 4 March 1993 is shown in Figure 5. The ozone concentration is presented as ozone partial pressure (P3) in mPa. The balloon burst at about 27.5 km altittude (17 hPa), just after detecting a maximimum ozone concentration of 12.6 mPa near an altitude of 25.8 km (22 hPa).

It is interesting to compare the measured ozone profile with one obtained at around the same time of the year (in northern hemisphere) at a similar latitude to see whether similar features can be identified. Based on the annual "Catalogue of Ozone Stations and Catalogue of Ozone Data" and the bi-monthly "Ozone Data for the World" published by the Atmospheric Environment Service of Canada in co-operation with the World Meteorological Organization (WMO), an ozone profile of Naha (latitude 26.1°N, longitude 127.4°E), Okinawa, Japan, measured at 06 UTC on 17 February 1993 is selected for comparison (Atmospheric Environment Service, 1993).

As only data pertaining to standard and significant pressure levels are available for the Naha profile, compatible data were extracted from the Hong Kong profile for the comparison (Figure 6). It is apparent that both profiles reveal similar features which are well documented, (*e.g.* see Junge, 1963): (a) a gradual decrease in the ozone partial pressure with altitude (except near the ground level) to less than 1 mPa (P3) at around 150 hPa despite irregular changes in between; and (b) a pronounced increase in the

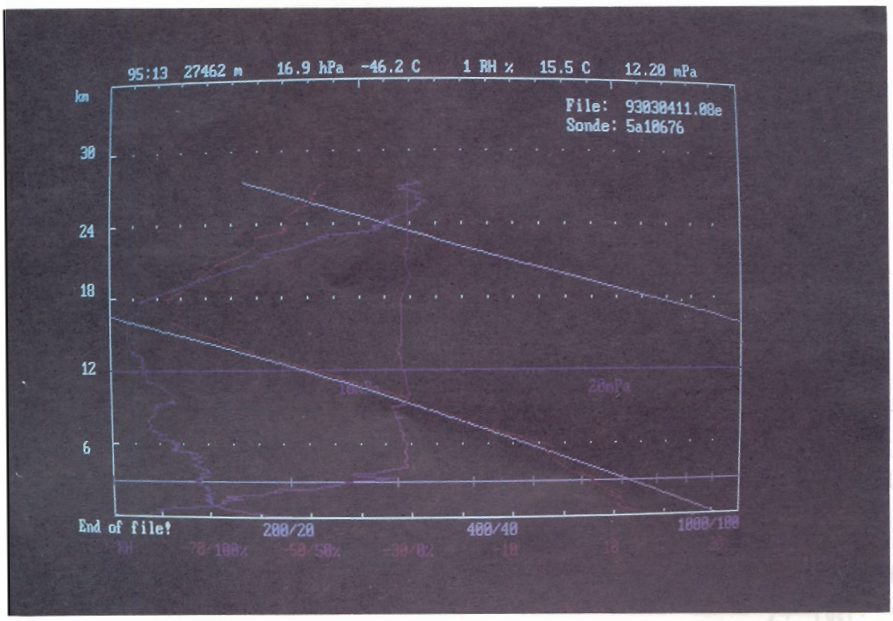

Figure 5 Real-time display of the vertical profiles of ozone concentration (blue), pressure (white), temperature (red) and humidity (pink) measured at 03 UTC on 4 March 1993.

and (b) a pronounced increase in the ozone partial pressure with altitude in the lower stratosphere to maximum values exceeding 12 mPa (P3) above the 30 hPa level. Unfortunately, due to balloon burst at about 17 hPa for the Hong Kong ascent, it is not certain whether the maximum value detected near 22 hPa is really the absolute maximum of the entire profile. Nevertheless, it is obvious that the maximum ozone level for the Naha ascent (13.3 mPa (P3) near 26 hPa) is at least a couple kilometres lower than that for the Hong Kong ascent (12.6 mPa (P3) near 22 hPa). It is also interesting to note that apart from the peak near 26 hPa, the Naha ascent also reveals local maxima between 50 and 100 hPa. These local maxima are not apparent on the Hong Kong ascent. Beyond these observations, more data will have to be accumulated for more detailed and quantitative analysis in order to understand the characteristics of the ozone profile over Hong Kong (*e.g.* the cause of the low ozone concentration near the ground surface at 03 UTC on 4 March 1993).

Scheduling of Radioactivity and Ozone Soundings

After the DigiCORA system becomes operational, radioactivity soundings will be made once every quarter to obtain background radiation profiles under different meteorological conditions. In the event that accidental release of artificial radioactivity occurs, additional soundings can be made to determine whether there is any significant increase in the radiation levels in the atmosphere over Hong Kong.

The Royal Observatory intends to make routine ozone soundings once a month. Since ozone sounding stations which carry out systematic measurements of vertical ozone distribution within the framework of the Global Ozone Observing System (GO3OS) are few and far between in this part of the world, (WMO, 1991), it is expected that data collected in Hong Kong can help to fill the data gap and contribute to better understanding of the global ozone distribution. In particular, the Royal Observatory will step up its ozone sounding activities between December 1993 and February 1994 in support of the Pacific Exploratory Mission (PEM-West) project involving the deployment of an instrumental DC-8 aircraft from the U.S. National Aeronautics and Space Administration (NASA) to measure trace gas concentrations in the atmosphere over the western Pacific. Further information on PEM-West can be found in NASA's booklet "Global Tropospheric Experiment" which is available from NASA Headquarters, Washington, D.C., U.S.A.

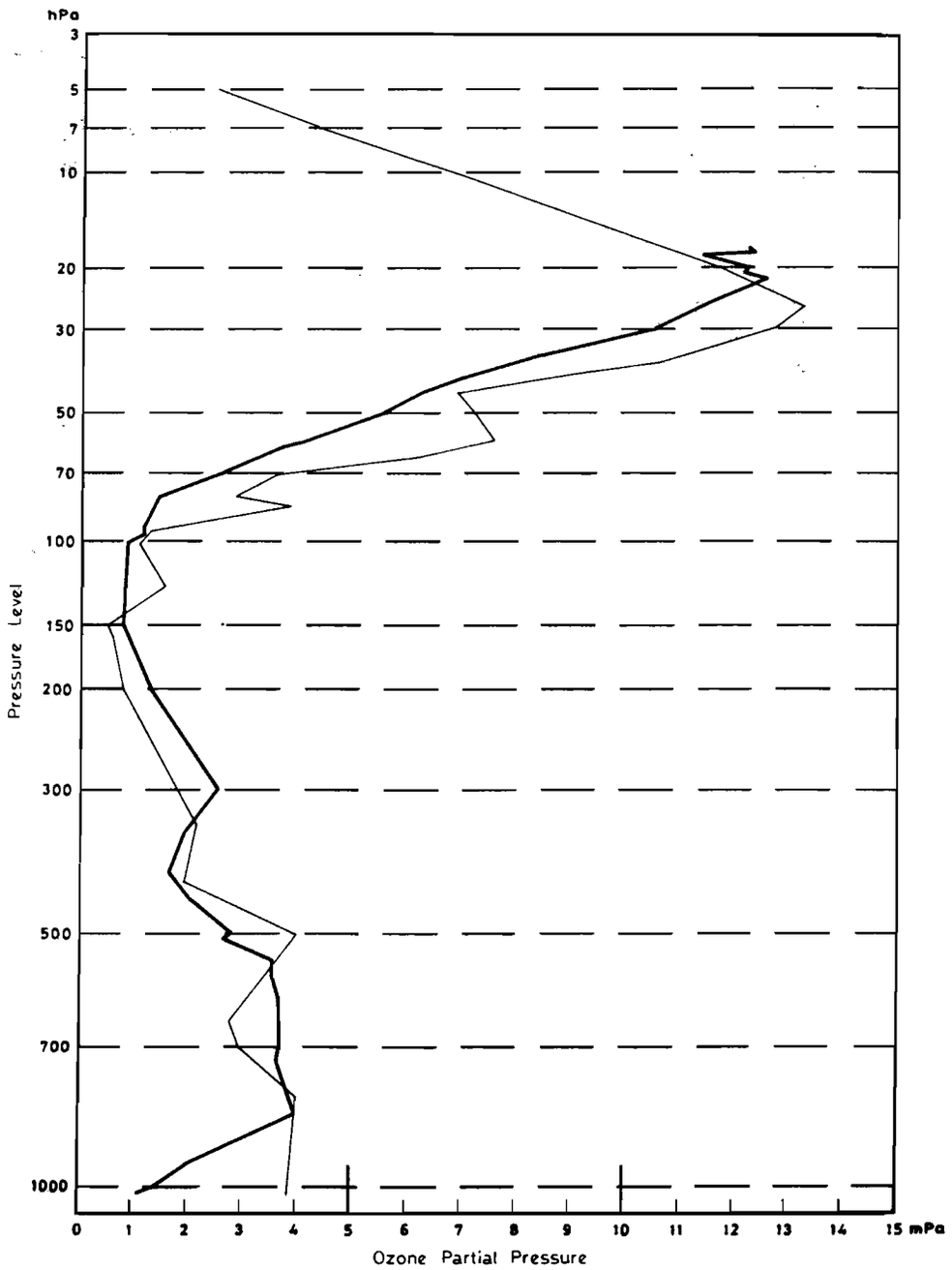

Figure 6 Vertical profiles of ozone concentration measured in Hong Kong at 03 UTC on 4 March 1993 (thick line), and Naha, Okinawa at 06 UTC on 17 February 1993 (thin line).

References

ATMOSPHERIC ENVIRONMENT SERVICE, 1993: *Ozone Data for the World: January-February 1993*, Vol. 34 No. 1. World Ozone Data Centre, Atmospheric Environment Service, Canada.

JUNGE, C.E., 1963: *Air Chemistry and Radioactivity*. International Geophysics Series Volume 4, Academic Press, New York and London, 382pp.

NASA, 1989: *Global Tropospheric Experiment: Probing the Chemistry/Climate Connection*, NASA Headquarters, Washington, DC, USA, 24pp.

VAISALA, 1992: *DigiCORA MW 11 and Marwin MW 12 User's Guide 8.1*, Vaisala OY, Helsinki, Finland.

VAISALA, 1993a. *Radioactivity Sonde User's Guide*, Vaisala OY, Helsinki, Finland.

VAISALA, 1993b. *Ozonesonde OES User's Guide*, Vaisala OY, Helsinki, Finland.

WORLD METEOROLOGICAL ORGANIZATION, 1991: *REPORT of the First Meeting of the Ozone Research Managers of the Parties to the Vienna Convention for the Protection of the Ozone Layer (Geneva 13-15 March 1991)*. WMO Global Ozone Research and Monitoring Project Report No. 23, World Meteorological Organization, Geneva.

News and Announcements

This section is intended for dissemination of news and announcements by the Society or any of its members. If members wish to relay any news or make any announcement of interest to members which is related to the aims of the Society they should mail or fax such information to the Editor-in-chief along with their name(s) and membership number(s).

EIGHTH RESEARCH FORUM

The Eighth Research Forum on the subject of *Localized Meteorological Phenomena in Hong Kong* will be held on Saturday 11th December, 1993 at the Hong Kong University of Science and Technology. Further details will be announced via regular newsletters.

FIFTH HONG KONG METEOROLOGICAL SOCIETY ANNUAL GENERAL MEETING AND NINTH RESEARCH FORUM

The Fifth Annual General Meeting of the Hong Kong Meteorological Society will be held on Saturday 12th March, 1994. The Ninth Research Forum will also be held on the same day in conjunction with the fifth Annual general Meeting of the Society. Further details of the meeting and the Research Forum will be announced via regular newsletters as they become available.

CUHK PUBLIC TALKS

The Department of Physics and the Centre for Environmental Studies have the pleasure to announce a series of public and non-technical talks principally in Cantonese on *Meteorology and Environment* by Professor LAU Ngar-cheung of the Geophysical Fluid Dynamics Laboratory and Department of Atmospheric and Oceanic Sciences, Princeton University, NJ, USA.

Professor Lau obtained his BSc in Physics from CUHK (1974) and his PhD in Atmospheric Sciences from the University of Washington 1978). Since then he has served the Geophysical Fluid Dynamics Laboratory of Princeton University. He has broad interests in atmospheric sciences. In particular, he is an expert in the analysis of the atmospheric circulation using both observational data and output from climate models, and area in which he has made important contributions. He will be visiting the department of Physics at CUHK from 27 November to 27 December 1993 as an C.N. Yang Visiting Fellow.

The talks are scheduled at the Science Centre of CUHK from 3:30 to 4:30 pm on the following dates in December, 1993:

2nd: Weather and Climate Variations - An Overview;

3rd: Atmospheric Greenhouse Warming;

8th: Ozone Hole in the Stratosphere;

13th: El Nino and Global Weather;

17th: Asian Monsoon and Local Weather.

JOINT SOCIETY SEMINAR WITH ROYAL OBSERVATORY

During his stay in Hong Kong Professor Ngar-Cheung LAU of Princeton University has kindly consented to present a technical seminar to be jointly organized by the Society and the Royal Observatory. The seminar on the topic *The Relative Roles of Tropical and Extratropical Sea Surface Temperature Anomalies in Atmospheric Variability* will be held on Monday, 20th December, 1993 at 3:30 pm. The venue will be the Conference Hall of the Royal Observatory, Hong Kong.

CONFERENCE PROCEEDINGS

Second International Conference on East Asia and Western Pacific Meteorology and Climate, September 7-10, 1992, Hong Kong

The Proceedings of the Second International Conference on East Asia and Western Pacific Meteorology and Climate have been published by World Scientific Publishing Company of Singapore. The conference was sponsored by the Hong Kong Meteorological Society with support from the University Corporation for Atmospheric Research, and was held from September 7-10, 1992 in Hong Kong. The Proceedings, edited by W.J. Kyle and C.P. Chang, contains papers presented by members of the Society and others at the conference.

1993 ATLANTIC BASIN SEASONAL HURRICANE FORECAST

from Bill Gray, Colorado State University

Information received through 3 June 1993 indicates that the 1993 hurricane should overall be about an average season with 7 hurricanes, 11 named storms of at least tropical storm intensity, a total of about 25 hurricane days, 55 named storm days and a Hurricane Destruction Potential (HDP) of 65. It is also expected that there should be two intense or major hurricanes of Saffir/Simpson intensity category 3, 4 or 5 and about 3 intense hurricane days.

The author's early June Atlantic seasonal hurricane forecast is based on the current values of indices derived from two global and three regional scale predictive factors which the author and colleagues have previously shown to be statistically related to seasonal variations of hurricane activity. The five predictive factors are:

(a) The Stratospheric Quasi-Biennial Oscillation (QBO) influence.

This refers to east-west stratospheric winds which circle the globe over the equator. On average, there is nearly twice as much Atlantic basin hurricane activity during seasons when equatorial relative winds at 30 hPa and 50 hPa (23 and 20 km altitude respectively) are westerly as compared to when they are easterly. During the 1993 season, these QBO winds will be from a westerly direction. This will be an enhancing influence on this season's hurricane activity.

(b) El Nino Southern Oscillation (ENSO) influence.

The effects of a moderate or strong El Nino warm water event in the eastern equatorial Pacific acts to reduce Atlantic basin hurricane activity. By contrast, seasons with cold sea surface temperature, or La Nina years, typically have enhanced hurricane activity. It is expected that the current El Nino event holding well through May will be weakening over the next three months and will not be a major inhibiting influence on this season's hurricane activity.

(c) African Rainfall (AR) influence.

Atlantic intense (category 3-4-5) hurricane activity is enhanced during those seasons when the Western Sahel and Gulf of Guinea regions of West Africa had above average late summer and fall precipitation during the previous year (*i.e.* in this case during fall of 1992). Hurricane activity is typically suppressed if the prior fall rainfall in these two regions has been below average. Conditions last year (1992) were dry and our forecast (Landsea *et al.* 1993) is for quite dry conditions this year. This should be a reducing influence on this season's intense hurricane activity.

(d) West Africa west-to-east surface pressure and temperature gradient influence.

Anomalous west-to-east surface pressure and surface temperature gradients across West Africa from February through May are strongly correlated with the hurricane activity which follows later in the year. Pressure and temperature gradients between February and May of this year were such as to indicate a somewhat below average hurricane season.

(e) Caribbean Basin Sea Level Pressure Anomaly (SLPA) and Upper Tropospheric (12 km) Zonal Wind Anomaly (ZWA) influence.

Negative anomalies imply an enhanced seasonal hurricane activity while positive values imply suppressed hurricane activity. April-May 1993 values of SLPA were quite negative while ZWA were only slightly positive. These effects indicate an enhancement of hurricane activity.

Table 1 shows the forecast of the amount of hurricane activity to be expected in the Atlantic basin in 1993. Table 2 compares this early June 1993 forecast to the late November 1992 forecast. Note that less intense hurricane activity is now projected. The November 1992 forecast anticipated cold ENSO conditions to be in place during the heart of the 1993 season in contrast to the slightly warm conditions now expected.

Table 1: 1993 Atlantic Basin Seasonal Forecast Values and the Percent of the Longterm (1950-1992) Average.

	Forecast	% of average
named storms (N)	11	119
named storm days (NS)	55	119
hurricanes (H)	7	122
hurricane days (HD)	25	107
intense hurricanes (IH)	2	93
intense hurricane days (IHD)	3	65
hurricane destruction potential (HDP)	65	94
net tropical cyclone activity (NTC)	95%	95%

Table 2: Comparison of early June 1993 and late November 1992 Seasonal Predictions.

	Forecast 11/92	6/93	diff.
named storms (N)	11	11	0
named storm days (NS)	55	55	0
hurricanes (H)	6	7	+1
hurricane days (HD)	25	25	0
intense hurricanes (IH)	3	2	-1
intense hurricane days (IHD)	7	3	-4
hurricane destruction potential (HDP)	75	65	-10
net tropical cyclone activity (NTC)	--	95%	--

Discussion: This is the tenth season that the author has made an Atlantic Basin seasonal hurricane forecast. It is also one of the most difficult to forecast due to the uncertainty concerning the resurgence of warm El Nino conditions in April and May. The author and most El Nino researchers did not anticipate this recent warming. However, the author does not believe that these warm sea surface temperature conditions will persist through the height of the hurricane season from mid-August through mid-October. Rather, a steady cooling is anticipated in the next 3-4 months. There is a difference of opinion among El Nino experts as to the rapidity of this cooling. Verification of 1993 forecasts and a forecast for 1994 will be issued in late November.

Background material:

Gray, W.M. C.W. Landsea, P. Mielke and K. Berry, 1992: Predicting Atlantic basin seasonal hurricane activity 6-11 months in advance. *Weather and Forecasting*, **7**, 440-455.

Gray, W.M. C.W. Landsea, P. Mielke and K. Berry, 1993: Predicting Atlantic basin seasonal tropical cyclone activity by 1 August. *Weather and Forecasting*, **8**, 73-86.

Landsea, .W., W.M. Gray, P.W. Mielke and K. Berry, 1993: Predictability of seasonal Sahelian rainfall by 1 December of the previous year and 1 June of the current year. *Preprints of* 20th Conference on Hurricane and Tropical Meteorology, San Antonio, Amer. Meteor. Soc., 473-476.

FORECAST FOR 1993 JUNE TO SEPTEMBER RAINFALL FOR NORTH AFRICA'S SAHEL

from: Chris Landsea, Colorado State University

The rainy season in North Africa's Sahel occurs almost exclusively during the months of June through September when the ITCZ reaches its farthest northward extension. The Sahel is defined here as the North African region between 10 and 20 degN. It is the area that has experienced numerous devastating droughts within the last two decades. This report provides a seasonal forecast for the Sahel based upon data available at the start of the rainy season.

Because of rainfall variability within the Sahel, a

homogeneous index of precipitation should not be utilized for the entire Sahel. Instead, three smaller subregions are organized within which precipitation shows similar year to year behaviour. These regions are the West, Central and East Sahel. The West Sahel extends from the Atlantic coast to 6 degW including portions of the countries of Mauritania, Senegal, Gambia, Guinea-Bissau, Guinea and Mali. The Central Sahel is the region from 6 degW to 26 degE and includes parts of Mali, Burkina Faso, Ghana, Togo, Benin, Niger, Nigeria, Cameroun, Chad, Central African Republic and Sudan. The East Sahel reaches from 26 degE to the Red Sea and is composed of parts of Sudan, Ethiopia, Eritrea and Djibouti.

The forecasting techniques are detailed in full in Landsea *et al.* (1993) and Gray *et al.* (1992, 1993). This statistical model utilizes the years 1950 to 1991 in a cross-validated (or jackknife) procedure that allows the independent testing of the individual years to test the skill of the model (for example, the year 1968 was tested by using the years 1950-1967 and 1969-1991 as the developmental data set). We use a Least Absolute Deviations (LAD) regression instead of the traditional Ordinary Least Squares (OLS) multiple regression. LAD is selected over OLS in that LAD is based upon minimizing the absolute differences between predicted and observed instead of the square of that value. Thus outliers do not overly influence the prediction equations. There are 13 predictors that are arranged in to 3 groups of similar predictors. The three groupings are: 1) the phase and magnitude of the stratospheric Quasi-Biennial Oscillation (QBO); 2) North African surface data; and 3) El Nino/Southern Oscillation (ENSO) / Caribbean basin conditions and their time change.

The individual predictors and their values to be used as input for the 1993 forecast are the following:

GROUP 1:
U winds at 50 hPa = -4 m s^{-1}
U winds at 30 hPa = -2 m s^{-1}
|U50-U30| = 2 m s^{-1}

GROUP 2:
Rs (previous year Aug-Sep West Sahel rainfall) = -0.95 Std. Devs.
Rg (previous year Aug-Nov Gulf of Guinea rainfall) = -0.90 Std. Devs.
Del-P (Feb-May anomalous pressure gradients) = -0.65 Std. Devs.
Del-T (Feb-May anomalous temperature gradients) = -0.20 Std. Devs.

GROUP 3:
SLPA (Apr-May Caribbean basin pressure anomalies) = -0.90 hPa
ZWA (Apr-May Caribbean basin 200 hPa zonal wind anomalies) = 0.5 m s^{-1}
SOI (Apr-May Southern Oscillation Index) = -1.15 Std. Devs.
SSTA (Apr-May eastern equatorial Pacific SST) = 1.45 degC
Del-SOI (Apr-May minus Jan-Feb SOI) = 0.20 Std. Devs.
Del-SSTA (Apr-May minus Jan-Feb SSTA) = 1.25 degC

Given these values for the predictors based upon information available to us at CSU by 4 June, the statistical model predicts values of:

	A	B	C
West Sahel	-1.61	-1.17	-0.72
Central Sahel	-0.80	-0.92	-1.04
East Sahel	-0.88	-0.38	+0.14

Std.Devs. The three sets are based on using: A: the above ENSO values; B: one/half ENSO values. and c: zero ENSO values.

Strictly using this model would be to use the first (A) column results. However, it is likely that the current moderate ENSO warm event (El Nino) as suggested by the SSTAs, SOI, and the change of SSTA and SOI, will not continue and will begin to reverse. The second (B) column presents rainfall values that result from assuming one half the current ENSO values. These may be more representative of those to be experienced during the height of the rainy season - August. Also note that while the West and especially the East Sahel show strong changes in the predicted rainfall with weaker to zero warm event conditions, the Central Sahel is nearly invariant to ENSO changes.

Besides the forcing of warm event ENSO toward drought conditions, the dry values forecasted are also due to very unfavourable predictors in the African surface data group and moderately favourable conditions in the QBO group (though this is the weakest predictive group).

Thus the "official" forecast that we believe is most likely to occur is for the following:

West Sahel: -1.20 Std.Devs. (3rd driest year since 1950)
Central Sahel: -0.90 Std.Devs. (8th driest year since 1950)
East Sahel: -0.40 Std.Devs. (17th driest year since 1950)

The amount of skill suggested by our hindcast tests indicate that for the West we should be able to forecast about 62% of the variance in the seasonal rainfall, 60% in the Central, and 46% in the East (Landsea *et al.* 1993).

Note that the forecast presented here is very similar to one issued by the United kingdom Meteorological Office (1993). Their prediction for the Sahel (for July to September rainfall throughout the entire area) is for "VERY DRY" (the lowest quintile) with moderate confidence.

A verification of this report will be done by late November of this year along with an extended range outlook for the Sahel rainy season of 1994.

REFERENCES

Gray, W.M. C.W. Landsea, P. Mielke and K. Berry, 1992: Predicting Atlantic basin seasonal hurricane activity 6-11 months in advance. *Weather and Forecasting*, **7**, 440-455.

Gray, W.M. C.W. Landsea, P. Mielke and K. Berry, 1993: Predicting Atlantic basin seasonal tropical cyclone activity by 1 August. *Weather and Forecasting*, **8**, 73-86.

Landsea, .W., W.M. Gray, P.W. Mielke and K. Berry, 1993: Predictability of seasonal Sahelian rainfall by 1 December of the previous year and 1 June of the current year. *Preprints of* 20th Conference on Hurricane and Tropical Meteorology, San Antonio, Amer. Meteor. Soc., 473-476.

United Kingdom Meteorological Office, 1993: Preliminary experimental forecast of 1993 seasonal rainfall in the Sahel and other regions of tropical North Africa. Report issued May 12, 1993, 3 pp.

TOPEX/POSEIDON

from: Ron Baalke, NASA/JPL, Pasadena

NASA's Jet Propulsion Laboratory and the Centre National d'Etudes Spatiales (CNES), the French space agency, are turning their scientific sights on Earth with a joint satellite mission designed to map the circulation of the world's oceans.

The Ocean Topography Experiment, or Topex, has been combined with France's Poseidon mission. Together, Topex/Poseidon satellite is the most sophisiticated attempt yet to measure and map sea level from space. It was launched on August 10, 1992 by an Ariane 42P booster rocket from the Arianespace Guiana Space Center in Korou, French Guiana.

Designed for a three- to five-year mission, Topex/Poseidon's primary science goal is to improve our understanding of how the oceans circulate. Such information will allow oceanographers to study the way the oceans transport heat and nutrients and how the oceans interact with weather patterns. Such studies will increase our understanding of the ocean's role in global change.

In the past, oceanographers have studied the sea from ships. This provided only a snapshot of the oceans' character because the ships took spotty measurements from fixed locations. Topex/Poseidon will provide a long-term, coherent, panoramic picture of the oceans. Such global information offers potential societal benefits such as improved long-range weather forecasting.

It will also aid in efforts to predict phenomena such as El Nino. Scientists have analyzed a prominent Kelvin wave which has appeared in Topex/Poseidon altimetry data. The scientists, at the Naval Research Laboratory, Stennis Space Center, Mississippi, report that their analysis of the data, as well as measurements taken by tide gauges and buoys, confirms that the Kelvin wave pulse which they predicted in February 1993 arrived at the South American coast as they anticipated.

Mission overview

The main instrument on the Topex/Poseidon satellite is a radar altimeter. This device is similar to ones that were flown on NASA's GEOS 3 satellite in 1975, on Seasat in 1978 and on the US Navy's Geosat in 1985.

As Topex/Poseidon orbits the earth, the altimeter bounces radar signals off the ocean's surface. The device records the time it takes the signal to return to the satellite and that gives it a precise measurement of the distance between Topex/Poseidon and the sea surface.

This data will be combined with measurements from other instruments that pinpoint the satellite's exact location in space. Scientists will then be able to produce a detailed map of ocean topography, or sea level relative to the earth's center. Sea level is directly related to ocean currents, eddies and other features of the ocean surface. When they examine the influence of the

earth's gravity field on sea level, researchers will also be able to study major features of the ocean floor. Information contained in the radar return signals can also be used to calculate wave height and wind speed, two elements that are important for monitoring the global sea state.

Planning by NASA and CNES calls for the United States to provide the satellite, altimeter, a microwave radiometer, an experimental satellite tracking receiver and various spacecraft subsystems. The French will supply the launch vehicle and two other instruments - a solid-state altimeter and a Doppler tracking receiver.

In 1987, an international team of 38 principal investigators was selected to participate in the Topex/Poseidon mission through a joint US-French announcement of opportunity. These scientists been working closely with the project to refine the mission design and scientific plans. After launch they will conduct a wide range of oceanographic and geophysical studies to accomplish the mission science goals.

Topex/Poseidon will complement other important oceanographic experiments planned for the 1990s:

The European Remote Sensing Satellite (ERS-1), launched by the European Space Agency, carries an altimeter and a scatterometer in addition to other instruments. The altimeter, when used in conjunction with the Topex/Poseidon data, will increase the sampling and coverage area. The scatterometer's measurements of global wind speed and direction, together with the altimetric sea-level measurements, will help scientists study how winds produce ocean currents and waves.

The NASA Scatterometer (NSCAT) is a JPL-managed instrument scheduled for launch aboard the Japanes Advanced Earth Observing Satellite (ADEOS) in February 1995. NSCAT will make frequent measurements of wind speeds and direction over the global ocean.

Oceanographers from around the world will also conduct studies using Topex/Poseidon data as part of the World Ocean Circulation Experiment (WOCE) and the Tropical Oceans Global Atmospheres Experiment (TOGA). these decade-long programs are sponsored by the World Climate Research Program.

Satellite design

Topex/Poseidon will orbit the earth at a relatively high altitude of 830 miles (about 1,340 km). This will minimize atmospheric drag on the spacecraft, reduce the influence of errors in measuring earth's gravity field, and simplify maneuvers needed to maintain the orbit position. The satellite orbit will be inclined 66 degrees from earth's equator.

The satellite's position in space must be known as precisely as possible in order to produce extremely accurate maps of sea level. Special laser and radio tracking on the ground will pinpoint Topex/Poseidon's position to within five inches (13 cm). By comparison, the orbit of Seasat was known to an accuracy of 20 to 40 inches (50 to 100 cm).

The NASA radar altimeter will operate at two frequencies, 13.6 and 5.3 gigahertz. Measurements of the same ocean area taken at both frequencies will help correct for path-delay errors caused by electrons in the ionosphere. A microwave radiometer, built by JPL, will measure radiation emitted from water vapor between the satellite and the ocean. This will be used to correct for path-delay errors caused by atmospheric water vapor.

The French space agency will provide an experimental solid-state altimeter on board the satellite. This altimeter operates at the single frequency of 13.65 gigahertz. The two altimeters will share the same antenna with the NASA altimeter being turned off a small part of the time so the French instrument can operate without interference.

The French will also provide a new radio-tracking system that will measure the position and velocity of the spacecraft. It is called Doppler Orbitography and Radiopositioning Integrated by Satellite (DORIS) and is a dual Doppler receiver which operates with a network of 50 uplink ground stations. DORIS will be used with the laser tracking system.

The United States is conducting a Global Positioning System precision orbit determination experiment along with this mission to test a new high-precision tracking system. A GPS receiver receives signals from the constellation of Navstar satellites established under the GPS program. Tracking information is sent to the ground for processing in the test ground operations system.

Mission benefits

The results of the scientific studies using data from Topex/Poseidon will increase our understanding of the ocean's role in global change and are expected to provide information about specific environmental problems.

Carbon dioxide: The burning of fossil fuels, combined with deforestation, is causing a significant increase of carbon dioxide in the atmosphere. This could ultimately produce catastrophic warming of the earth. The impact appears to be critically dependent upon how fast carbon dioxide is absorbed by the ocean and how efficiently the ocean interacts with the atmosphere to slow down the potential global warming. Both factors rely, in part, on ocean currents. Detailed knowledge of ocean circulation could help scientists determine what threat increased carbon dioxide in the atmosphere may pose for earth's future.

Weather forecasting: Weather patterns in North America are heavily influenced by events over the ocean -- in this case, the Pacific. Analysis of Topex/Poseidon data will eventually help forecasters predict general weather trends a season ahead, enabling the agriculture industry to adjust crop selection. Such predictions would also benefit energy planning in the Northeast United States by forecasting unusually cold or warm winters.

Offshore oil, mining, and coastal power plants: Such facilities must be designed to withstand severe wave and storm surges, such as those caused by hurricanes along the United States' Gulf Coast. Observations from Topex/Poseidon will provide information for better planning in the location and construction of oil rigs, drill ships, mining operations and coastal nuclear power plants.

Seabed disposal of dangerous wastes:
the safety of such disposal depends partly on the rate at which currents may carry potentially hazardous leakage from disposal sites toward fishing grounds and coastal areas.

REPORT OF THE WORKSHOP ON CLIMATE CHANGE AND THE EL NINO - SOUTHERN OSCILLATION (ENSO)

The Workshop on Climate Change and the El Nino - Southern Oscillation was hosted by the Climate Group of the Bureau of Meteorology Research Centre, Melbourne, Australia, on Monday 31 May and Friday 4 June, 1993. This meeting complemented the Western Pacific Workshop on Seasonal to Interannual Climate Variability which was held in the Bureau of Meteorology on the Tuesday to Thursday of the same week. Financial support for the Climate Change workshop was provided by the Climate Change Program of the Australian Department of the Environment, Tourism, Sport, and Territories, and by the Bureau of Meteorology Research Centre. Over 30 scientists from Australia, New Zealand and USA participated.

The workshop theme was similar to that of two previous meetings. The first of these, on past changes in the El Nino - Southern Oscillation, was held in Boulder, Colorado, USA in May, 1990. Papers presented at that meeting were published in *El Nino: Historical and Paleoclimatic Aspects of the Southern Oscillation*, edited by Henry Diaz and Vera Markgraf, and published by Cambridge University Press in 1992. A meeting on *ENSO and Climate Change* was held in Bangkok, Thailand in November, 1991. A report of this meeting was published by the United Nations Environment Program and the Environmental and Societal Impacts Group of the National Center for Atmospheric Research. The report included an assessment of the likelihood of changes in ENSO, under an enhanced greenhouse effect. The Melbourne workshop was intended to examine recent work to determine if the assessment prepared in Bangkok could be refined.

This short report includes the workshop program, brief summaries of the presentations, and summaries of the discussion sessions. A fuller version of the report, which also includes one-page abstracts of the presentations, can be obtained from the Administrative Officer, BMRC, PO Box 1289K, Melbourne 3001, Australia, while copies last.

Program

Monday 31 May, 1993

0900-0915 Welcome & opening (N. Nicholls)

Past variations in ENSO behaviour - Historical data

0915-0945 Stability of ENSO-climate relationships (C. Ropelewski & X. Wang)
0945-1015 20th century fluctuations in ENSO (R. Allan)
1015-1030 Changes in the relationship between ENSO and Queensland rainfall: 1891 to 1986 (J. Lough)
1030-1045 ENSO & sea level - 20th century variations (W. Mitchell)

1045-1115 Coffee

Past variations in ENSO behaviour - Proxy data

1115-1145 Tropical and extratropical ENSO signals in long tree-ring records (E. Cook & R. D'Arrigo)
1145-1215 Historical aspects of the ENSO: Information from massive corals (J. Lough)
1215-1245 Climate reconstruction in monsoonal Australia (R. Wasson & P. Crapper)
1245-1300 Association between tree ring-index time series and ENSO (J. Murphy)

1300-1400 Lunch

Model variations in ENSO behaviour

1400-1430 Tropical Pacific interannual variability and CO_2 climate change (G. Meehl)
1430-1500 The influence of mean climate state on tropical interannual variability in a coupled model (A. Moore)
1500-1530 Low-order coupled models (R. Kleeman)

1530-1600 Coffee

1600-1630 The CSIRO AGCM (I. Smith)
1630-1645 The BMRC ACGM (N. Nicholls, C. Frederiksen, R. Balgovind & P. Indusekharan)

User perspectives

1645-1715 ENSO and Climate Change: a grassland user's perspective (G. McKeon, S. Howden & D. White)

1900 Dinner

Friday 4 June, 1993

0900-0930 ENSO teleconnections in the eastern hemisphere over the past 500 years (P. Whetton & I. Rutherford)
0930-1000 Climate change & ENSO: The South Pacific (M> Salinger)
1000-1045 Discussion of presentations

1045-1115 Coffee

1115-1230 Discussion of presentations

1230-1400 Lunch

1400-1530 How might climate change affect the El Nino - Southern Oscillation?
1530-1600 Suggestions for future research

Summaries of presentations

Stability of ENSO-climate relationships
(C. Ropelewski & X. Wang)

* ENSO exhibits a higher frequency mode (2-7 year period) superimposed on decadal (and longer) variations.
* Weak ENSO signal around 1920-1940, just after minimum global temperature.
* Global sea surface temperature variability was lower soon after minimum global temperature.

20th century fluctuations in ENSO
(R. Allan)

* Pressure field exhibits weaker ENSO teleconnections during 1920-1940.
* Three distinct ENSO modes apparent in the pressure fields: 1/2. Interhemispheric (either northern hemisphere into southern hemisphere or vice versa); 3. Zonal (little meridional movement in the pressure anomalies).
* The zonal mode was dominant during 1920-1940.

Changes in the relationship between ENSO and Queensland rainfall: 1891 to 1986
(J. Lough)

* Weak Queensland-ENSO teleconnection 1915-1945, during which time rainfall was less variable and, on average, low.

ENSO & sea level - 20th century variations
(W. Mitchell)

* Coherent sea level variations along south coast of Australia are related to ENSO, and are the result of wind stress changes over the Southern Ocean.
* Data exists since 1880s and is being studied for long term changes.

Tropical and extratropical ENSO signals in long tree-ring records
(E. Cook & R. D'Arrigo)

* North Mexico tree rings show ENSO signal at about 3.8 yr period. This signal was strong 1790-1930 and weak around 1940.
* Java teak rings show ENSO signal at about 6 yr. This was strongest in early 20th century (record stops in 1929).
* The Great Barrier Reef coral fluorescence shows an ENSO signal at about 4yr, again strong in the early 20th century and weak in the 1940s.

Historical aspects of the ENSO: Information from massive corals
(J. Lough)

* Great Barrier Reef corals show periods with low and less-variable rainfall 1780-1810, 1828-1857, 1907-1936. It was wetter and more variable in Queensland in 1881-1910, 1751-1780, and 1951-1980.
* Tarawa corals (Cole *et al.*) show reduced rainfall variability 1920-1940.

Climate reconstruction in monsoonal Australia
(R. Wasson & P. Crapper)

* Magela Swamp (Northern Territory) shows increasing moisture from 2000 years ago to about 750 years ago. After 750 years ago possibly decreasing moisture.
* This long-term trend is out-of-phase with Quelccaya ice accumulation, but short-term fluctuations in ice accumulation and Northern Territory rainfall (associated with ENSO) are generally in phase.
* There has been no significant variation in large storms over the Great Barrier Reef over past 200 years (tropical cyclone activity in this area is closely related to ENSO).
* Frequency of floods over Northern Australia has been relatively constant until an increase in past 200 years.

Association between tree ring-index time series and ENSO
(J. Murphy)

* Java teak (extended to recent times) coherent with ENSO at 6 and possibly 12 year periods.
* Change in correlation of teak with ENSO since 1920, now strongest for teak lagging SOI.
* New Zealand trees positively correlated with SOI one season earlier.

Tropical Pacific interannual variability and CO_2 climate change
(G. Meehl)

* With increased CO_2 coupled model continues to exhibit ENSO-like variability in the tropics and effects are more intense (droughts and floods more extreme).
* Extratropical teleconnections change due to changed basic state.
* Nonlinear change in evaporation as sea surface temperature increases appears to be very important for ENSO in a warmer climate.

The influence of mean climate state on tropical interannual variability in a coupled model
(A. Moore)

* Coarse-grid coupled models simulate some forms of tropical interannual variability.
* This variability is sensitive to the mean sea surface temperature distribution and to differences between models.

Low-order coupled models (R. Kleeman)

* Hindcast experiments under current conditions indicate thermocline displacements are important for simulating ENSO so we need high resolution tropical Pacific coupled model with good thermocline depiction, if we are to use model to determine effects of climate change on ENSO.

The CSIRO AGCM (I. Smith)

* Little change in pressure patterns associated with ENSO, when global sea surface temperatures are increased, but precipitation teleconnections are more intense.

The BMRC ACGM (N. Nicholls, C. Frederiksen, R. Balgovind & P. Indusekharan)

* The GCM forced with observed sea surface temperatures reproduces SOI variations, except for the bias to low SOI over the past decade (during the period of warm global temperatures).
* Variability (peak-to-peak) of SOI not affected by imposing 1°C increase in global sea surface temperatures.

ENSO and Climate Change: a grassland user's perspective
(G. McKeon, S. Howden & D. White)

* The stability of ENSO teleconnections is important for the user of ENSO-related seasonal climate predictions.
* Use of seasonal climate predictions (by farmers for instance) can help them adjust incrementally to climate change.

ENSO teleconnections in the eastern hemisphere over the past 500 years
(P. Whetton & I. Rutherford)

* Broad-scale ENSO teleconnections have operated since at least the 18th century, but they were weak around 1920-1940.
* Little evidence before 1750 of ENSO teleconnections, although the data is poorer.

Climate change & ENSO: the South Pacific
(M. Salinger)

* Recent decadal changes in precipitation and central equatorial Pacific temperature is similar to that expected from recent changes in ENSO.

* But opposite sign in southwest Pacific temperatures (*i.e.*, the recent warming there is not due to changes in ENSO).

Summaries of Discussion Sessions

1. How might climate change affect the El Nino - Southern Oscillation?

A discussion session on the second day of the workshop addressed the question of how ENSO might change under enhanced greenhouse effect conditions. The scope of the discussion was limited to the scale of the climate changes expected from an enhanced greenhouse effect over the next few decades, *i.e.* global warming of perhaps 1°C. The discussion session focussed on revising the assessments made at the Workshop on ENSO and Climate Change held in Bangkok, Thailand, 4-7 November 1991, sponsored by the United Nations Environment Program and the Environmental & Societal Impacts Group at the National Center for Atmospheric Research. Participants at the Melbourne workshop considered that sufficient advances had been made in our understanding of the relationship between climate change and ENSO to justify revising the Bangkok assessments. The possible impact of an enhanced greenhouse effect on various aspects of ENSO was considered, as had been done in Bangkok. The notes below summarize the consensus reached at the meeting.

A clear caveat must be attached to the suggestions listed below. The participants at the meeting agreed that our understanding of ENSO is still far from complete, and the modelling of the phenomenon is still rather rudimentary. Much work is still required to refine and confirm the possible effects of climate change on ENSO, before they can be used in assessing societal or ecosystem impacts.

Will the El Nino - Southern Oscillation continue to occur? Very likely. Proxy climate evidence indicates that it has occurred under a variety of climate regimes. Model studies also suggest it will continue to operate under an enhanced greenhouse effect.

Will the frequency of El Nino episodes change? Possibly. Historical evidence suggests changes in the frequency of episodes has varied in the past, although the causes of such changes are not known.

Will the duration of El Nino episodes change?

Less likely. The duration of present-day events is clearly related to the annual cycle and the monsoon circulation and it seems unlikely this will alter dramatically under enhanced greenhouse conditions.

Will the El Nino - Southern Oscillation change in intensity? A model study suggested little change in the intensity of the sea surface temperature anomalies associated with ENSO under an enhanced greenhouse effect. There is, however, model and observational evidence suggesting increased precipitation variability under an enhanced greenhouse effect. This also seems likely on theoretical grounds due to the enhanced hydrological cycle likely to result from an enhanced greenhouse effect. This intensification of precipitation anomalies might occur even if the fundamental ocean-atmosphere oscillation does not intensify.

Will there be a systematic change in extratropical teleconnections? Likely, because changes in the background climate state resulting from the enhanced greenhouse effect will result in changes in teleconnections. It will be difficult, however, to distinguish these changes from those associated with the natural variability of the basic state.

2. Suggestions for future research.

The final session of the workshop addressed the question of what future research is both necessary and feasible to refine and confirm the suggestions about how the El Nino - Southern Oscillation might react to an enhanced greenhouse effect. The list below was not seen as exhaustive but it does indicate what participants saw as promising lines of research.

* Further empirical studies, with both instrumental and proxy records, are needed to separate decadal variability from interannual variability. This could lead to a better understanding of how slow climate variations affect the variability associated with ENSO.

* The period of the 1920s-1940s showed an apparent weakening of ENSO and its teleconnections and impacts. Some evidence presented at the workshop led to a tentative suggestion that this might be associated with rapid global warming around that time. Further work is needed to determine the likely causes of this weakening.

* Current models of ENSO need to be improved. Such models offer the best method for gauging the impact of an enhanced greenhouse effect on ENSO. At present some of these models are used in experimental predictions, but the accuracy of these predictions needs to be higher, if they are to

provide confident predictions on the interannual time-scale, as well as to gauge the effects of climate change.

* Theoretical studies of how to detect changes in the El Nino - Southern Oscillation are needed. The detection of such changes will require somewhat different strategies to the "fingerprint" strategies being developed to detect climate change per se.

* Model studies of the El Nino - Southern Oscillation during cooler periods are needed to validate and test hypotheses arising from paleoclimate studies.

* Increased emphasis on production of regional climate reconstructions from paleodata is needed. ENSO produces a specific regional pattern of interannual climate variations. This pattern, with regional paleoclimate reconstructions, could provide better information on past changes of the phenomenon.

* Paleo reconstructions of tropical sea surface temperatures, especially of the warm pool of the western equatorial Pacific, could provide important information about past changes in ENSO.

* Stochastic modelling of paleo and instrumental climate data is necessary to provide an understanding of past variations in behaviour of ENSO, and provide the necessary information to determine the significance of changes in the phenomenon.

Bill Kyle

Department of Geography & Geology

The University of Hong Kong

Hong Kong Weather Reviews

Climatological information employed in the compilation of this section is derived from published weather data of the Royal Observatory, Hong Kong and is used with the prior permission of the Director.

Review of winter 1992-93

Important climatological events

Taking the season as a whole Winter 1992-93 had near normal rainfall but was considerably milder than usual. The seasonal mean minimum temperature (15.4°C), seasonal mean temperature (17.2°C), and seasonal mean maximum temperature (19.5°C) were 1.1, 0.7 and 0.2°C respectively above the seasonal normals. However, each month was distinctly abnormal in at least one respect. December was one of the warmest on record and was also unusually humid. The monthly total rainfall was nearly two and a half times the December normal. All of these anomalies can be attributed to subdued winter monsoon activity during the month. January, by contrast, was atypically cold with the longest cold spell since 1887. Daily minimum temperatures were below 12°C for 16 and daily mean temperatures were below 12°C for 11 consecutive days following an intense surge of the winter monsoon on the afternoon of 14th. The month was also considerably wetter with 43 percent above normal rainfall. February, like December, was unseasonably mild due to the absence of cold air surges leading to one of the warmest Februarys on record. However, unlike December, the month was also very dry with only 1 mm or about 2 percent of the 1961-90 normal of 48.0 mm recorded.

Mean daily temperature	**17.2°C**	**(+0.7°C)**
Rainfall (provisional)	**100.9 mm**	**(102 %)**

December

After the dominance of the winter monsoon in November the circulation became subdued in December with only two northerly surges bringing short duration cold spells. Hence the month was one of the warmest since records began. The monthly mean minimum temperature of 17.4°C, mean temperature of 19.2°C, and mean maximum temperature of 21.4°C were respectively the second, third and tenth highest on record for December. The month was also unusually humid with fog being reported inside the harbour for the first time in December since 1955. Mean wet-bulb temperature (16.7°C), dewpoint temperature (14.9°C), and relative humidity (77%) ranked third, seven and tenth highest for the month. The dry spell which began in August also ended with monthly total rainfall of 66.4 mm being nearly two and a half times the 1961-90 normal of 27.3 mm. Most of this fell during an unseasonal period of wet weather after Christmas.

For the first twelve days of the month the weather was generally fine and mild. Traces of rain occurred on 2nd, 7th and 11th but otherwise it was dry. During this time there were three weak replenishments of the winter monsoon with easterlies freshening on 3rd, 8th and 11th. On all three occasions the associated temperature drops were insignificant. During a lull in the easterlies on 7th the maximum temperature reached 25.4°C, the high for the month. The weather became cloudier on 13th and easterly winds picked up that night. A major surge of colder northerly winds arrived on the evening of 14th with light rain occurring throughout the night and temperatures began to fall. With increasing cloudiness on 15th cold air advanced across the coast of south China lowering the temperature to the month's minimum of 11.7°C on the morning of 16th.

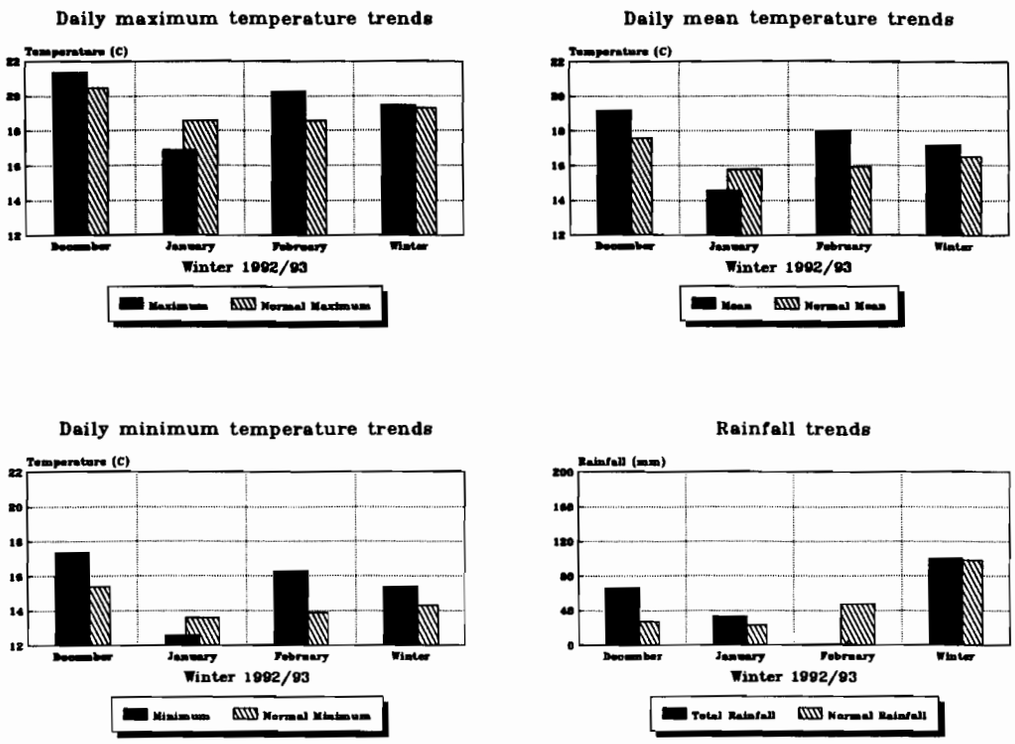

This cold period was short-lived as winds turned easterly. The arrival of this warm, moist airstream produced some light rain around midday on 20th and raised temperatures again to a high of 25.4°C on 21st. Easterlies freshened early on 22nd bringing cloudier conditions. A second northerly surge arrived on the morning of 23rd marking the beginning of a week-long cloudy spell. The cold spell culminated on 24th and strong easterly winds gave rise to cloudy and windy conditions with light rain patches on Christmas Day. The added moisture in the lower atmosphere produced continuous rain on Boxing Day with the total of 23.0 mm making it the wettest since records began. The rain ended the next morning but humid conditions under light winds remained for the next few days. Visibility reached a low of 900 metres in the harbour on the morning of 28th, the first time fog had been reported inside the harbour in December since 1955. On 29th easterlies picked up, clearing away the low-lying mist but bringing back persistent rain. A moderate northeast monsoon brought an improvement on 30th as drier air returned producing an easing of the rain and a slightly cooler night. However, sunny skies on 31st ensured a mild last day of the month and of the year.

Mean daily temperature	**19.2°C**	**(+1.6°C)**
Rainfall (provisional)	**66.4 mm**	**(243 %)**

January

A warm December was followed by a colder than usual January during which new records were set for a prolonged cold spell. For 16 consecutive days from 15th to 30th daily mean minimum temperatures were below 12°C and for 11 consecutive days from 15th to 25th daily mean temperatures were below 12°C the longest cold spell in January since 1887. The month was also notable for its 33.5 mm of rain, 43 percent above the normal of 23.4 mm for the month.

The year started with two weeks of relatively warm weather with mostly fine conditions interspersed with brief periods of cloud, light rain and slightly lower temperatures linked to weak replenishments of the winter monsoon. The first of these occurred on the night of 4th, a second in

the early hours of 8th. Both were short-lived and winds soon moved to the south-east bringing in warm, moist maritime air. Mist patches appeared on the evening of 8th and morning of 9th. The month's highest temperature of 23.7°C occurred on 10th. A third replenishment on the morning of 11th brought easterlies which persisted for the next two days so that the weather was noticeably cloudier with outbreaks of drizzle. These too moderated and veered to the southeast on the evening of 13th bringing yet more moist air to form mist inside the harbour on 14th. A cold front associated with an intense surge of the winter monsoon reached Hong Kong on the afternoon of 14th. The temperature started to fall that evening as the northerly winds strengthened marking the beginning of a prolonged cold spell which lasted till the end of the month. There was frequent light rain on 15th. By the morning of 16th temperatures had dropped by nearly 16°C from the maximum temperature on 14th of 21.3°C to 5.4°C, the lowest recorded during the month. With such low temperatures freezing conditions occurred on high ground with ice and glaze reported at Tai Mo Shan where temperatures dropped to -2.0°C. Although that day was sunny temperatures remained low as cold air poured south over the coastal areas. Cloud returned on 17th and light rain began that evening and continued to 19th. A northerly replenishment on 23rd ended a four day dry spell and brought 13.3 mm of rain on the first day of the Chinese New Year, an amount second only to the record of 15.8 mm set in 1911. Clouds began to clear on 24th as dry continental air became established in depth bringing fine conditions which persisted for the remainder of the month. Although the abundant sunshine produced mild daytime conditions the lack of clouds facilitated radiative cooling at night keeping minimum temperatures low especially in inland areas. Sub-zero temperatures were recorded at Ta Kwu Ling on 28th and there were reports of ground frost in the northern New Territories on the mornings of 29th and 30th. The dry air also mean that relative humidity values remained below 40 percent on 27th and 28th. By the last day of the month the cold spell had all but ended with winds turning easterly and cool, moister air beginning to affect the coast.

Mean daily temperature	**14.6°C**	**(-1.2°C)**
Rainfall (provisional)	**33.5 mm**	**(143 %)**

February

February was in sharp contrast to January with relatively cold conditions being followed by mild weather associated with the dominance of easterly monsoon and the absence of significant surges of cold northerly monsoon air. The monthly mean temperature of 18.0°C and the monthly mean minimum temperature of 16.3°C were both the fourth highest on record for the month. The month was also very dry with a total of only 1.0 mm of rain, about 2 percent of the normal of 48.0 mm. This made the month the seventh driest February on record.

Strong easterly winds produced cool and windy conditions on the first two days although it was generally fine and sunny. The monthly minimum temperature of 12.8°C was recorded on the morning of 2nd. On 3rd, winds moderated and turned southeasterly bringing in moister and warmer maritime air leading to an increase in temperature and cloudiness over the next few days. Cloudiness significantly increased on 6th with some drizzle and mist forming offshore overnight which thickened into fog the next morning. However, this soon lifted giving a sunny day as winds veered to the southwest. The easterlies freshened again early on 8th to bring cooler conditions, more mist and some light rain that evening and on 9th. Conditions improved on 10th and generally fine weather prevailed for the next week. During this time winds were generally easterly to southeasterly alternating in strength. Fresh to strong easterlies prevailed from 12th to 14th. Lulls occurred, bringing some morning mist, on 11th and 16th, the latter day recording the highest temperature for the month of 23.4°C. A fresh easterly airstream arrived on 17th, cloudiness increased on 18th and persisted till the end of the month. Some light rain was recorded on each of the three days 18th to 20th and mist returned on 19th as the air became more humid. This thickened to fog on the mornings of 20th and 21st which entered the harbour. The passage of a weak cold front on 22nd improved visibility and brought some light rain and a lowering of temperatures by three to four degrees by the next day as winds backed to the northeast. Easterlies returned in strength on 26th bring mist and drizzle which remained until the winds began to turn northerly again on 28th.

Mean daily temperature	**18.0°C**	**(+2.1°C)**
Rainfall (provisional)	**1.0 mm**	**(2 %)**

Review of spring 1993

Important climatological events

In sharp contrast to the very wet spring of 1992, spring 1993 was one of near-normal

precipitation and temperatures. The seasonal mean minimum temperature (20.5°C), and seasonal mean temperature (22.4°C) were 0.3 and 0.2°C respectively above the seasonal normals. The seasonal mean maximum temperature (24.8°C) was 0.2°C below the normal. Total rainfall of 523.7 mm was 96 percent of the seasonal average. The season started off with a milder, cloudier and more humid March characterized by the changeable conditions associated with alternation between late bursts of the winter monsoon and warm, humid, southerly airstreams. April was generally cooler and drier than normal due to a persistent, late spell of active northeast monsoon during the early part of the month. In terms of both temperature and precipitation, the weather of May was very typical with most of slightly above normal rainfall associated with the passage of monsoon troughs.

Mean daily temperature	**22.4°C**	**(+0.2°C)**
Rainfall (provisional)	**523.7 mm**	**(96 %)**

March

The mild conditions characteristic of February continued into March which was warmer, cloudier and more humid than normal. The weather for the month was typically springlike with spells of cooler weather brought by late bursts of winter monsoon interspersed with warm, sunny periods with southerly winds, times of humid conditions and fog and periods of unsettled weather. Overall rainfall for the month of 49.0 mm was 27 percent below the March normal of 66.9 mm.

The first few days of the month were cool and cloudy under the influence of the northeast monsoon. A weak northeast replenishment brought mist patches on the evening of 3rd and some light rain later that night. By 5th the weather turned fine and conditions warmed up the next day as the northeast monsoon weakened. The weather remained mainly fine for the next week apart from some mist on 7th and 8th associated with a fresh, moist easterly airstream. The easterlies freshened again on 12th giving windy, cloudy and cooler conditions on 13th. Light rain began that afternoon and persisted into 14th before dying out and giving some morning mist patches. A southwesterly airstream developed during 14th giving gusty winds and warmer weather on 15th although some light rain patches also occurred. The intrusion of moist, maritime air brought increased coastal fog patches on the morning of 15th and 16th. A cold front crossed the south China coast on the evening of 16th causing a deterioration in the weather with rain and thunderstorms lasting till the morning of 17th. Weather remained cloudy for the next three days with patches of light rain at night. Although winds were fresh from the east at first they turned more northerly bringing cold air to the coastal regions and lowering the temperature to the month's minimum of 11.3 °C on the morning of 19th. Winds veered to the east on 21st and then to the southeast on 23rd steadily raising temperatures again. With moist maritime airstreams coastal mist and fog occurred from time to time from 23rd to 27th. However, the sun broke through on 24th and fine, warm weather dominated the next four days after morning mist and fog lifted. The month's high temperature of 28.1 °C was recorded on 28th. Another cold front brought strong easterly winds early on 29th and with them cooler conditions. Light rain occurred at this time and again on the evenings of 30th and 31st. Although cloudy conditions prevailed winds turned southwesterly towards the end of the month and temperatures began to rise again.

Mean daily temperature	**19.4°C**	**(+0.9°C)**
Rainfall (provisional)	**49.0 mm**	**(73 %)**

April

April was cooler and cloudier than normal due to the late season activity of the northeast monsoon which particularly affected the first part of the month. The latter half of the month was milder and more humid with frequent mist and fog although late season surges again brought rain and thunderstorms. Although there were only seven rain-free days the total rainfall for the month was 16 percent below average with 136.3 mm.

The month began with mist and fog brought by a moist maritime airstream. This airstream also brought cloud and light rain patches for the first two days. The fog lifted on 3rd to give long sunny periods on that day and the next. Easterly winds strengthened on the morning of 5th as an easterly surge began. This brought increased cloudiness and light rain which became more persistent the next day. Winds turned northeasterly on the night of 6th bringing cooler air from inland. Temperatures dropped from a high of 27.9°C on 3rd to the month's minimum of 14.6°C on 7th as a consequence of this surge. Heavier

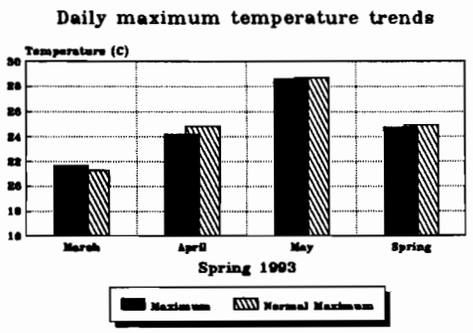

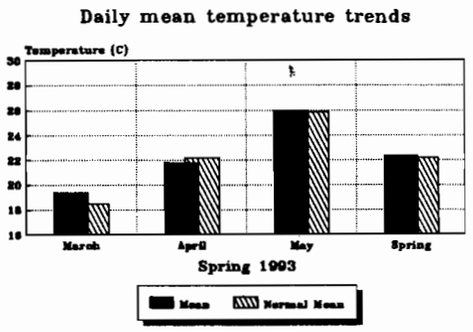

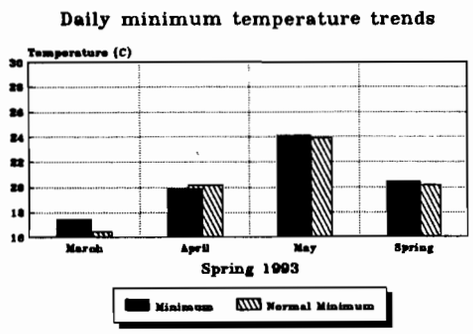

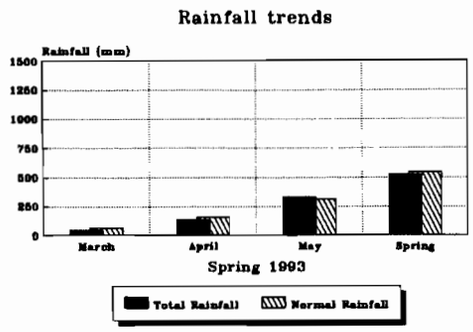

rain accompanied thunderstorms on the evening of 7th before winds veered to the east on the night of 8th. Continued replenishments of the northeast monsoon maintained fresh winds and relatively cool weather for the next 4 days. During this time drier, continental air was brought to the coastal regions and this gave fine and sunny weather from 12th to 16th. Easterly winds then freshened bringing increased cloud and light rain on the morning of 17th. Heavier rain and thunderstorms followed on 18th before rain eased off later that day. Clouds and mist on 19th thickened overnight to give widespread fog on the morning of 20th. Heavy rain and thunderstorms occurred that afternoon and evening giving the heaviest rain of the month. Although there was a lull during the night more rain and thunderstorms returned on 21st. Following these the increasingly active southwest monsoon brought showers in the morning but warmer and brighter conditions later during the next few days. A southeasterly airstream set in early on 25th bringing foggy conditions. This warming trend led to the month's highest temperatures of 29.8°C on that day. This was short-lived as a strong easterly airstream arrived late that afternoon. Between midday and midnight temperatures dropped nearly 10 degrees. The easterly surge also brought rain and thunderstorms that evening. The easterlies moderated on 26th and winds gradually turned southerly heralding a period of cloudy humid weather. Apart from 28th, which was fine, conditions were generally unsettled with rain developing on the night of 29th. The month ended with widespread thunderstorm activity associated with a trough marginally affecting Hong Kong.

Mean daily temperature 21.8°C (-0.4°C)
Rainfall (provisional) 136.3 mm (84 %)

May

The weather of May was typical of the season with mean temperature of 26.0°C being 0.1°C above normal and rainfall of 338.4 mm, just 7 percent above the May normal of 316.7 mm. Most of the month's rain was associated with the passage of monsoon troughs. In the first half of

the month each passage was followed by a weak surge of late-season northeast monsoon through the Taiwan Strait. A slow-moving trough in the second half of the month brought a period of prolonged rainy weather.

May began with heavy rain associated with the formation of a trough of low pressure which formed over Guangdong and moved south towards the coast. Heavy thunderstorms occurred in the early morning of 1st and on the afternoon of 2nd. Heaviest rain occurred in the Tsuen Wan and Shatin areas where over 200 mm was recorded. Rain eased off on 3rd following the passage and weakening of the trough. That evening easterly winds freshened bringing some light rain. The cloudy and humid conditions remained the following day with rain and thunderstorms in the morning, mist in the afternoon and evening and drizzle during the night. The month's low of 20.6°C was recorded early on 4th. Rain died out on 5th and the sun appeared briefly as the winds turned southeasterly. This brought fog that evening and for the next two mornings as moist maritime air moved in. Otherwise the weather was fine and sunny from 6th till early on 9th when another trough passed through. Weather deteriorated during the day with torrential rain and thunderstorms continuing to midnight. As before Tsuen Wan and Shatin received the heaviest downpours. Sunny periods reappeared on 10th but light rain began that night as easterly winds freshened. The following few days were mainly fine and sunny with morning fog. As another trough passed through early on 15th, easterly winds freshened and it became cloudy. This trough was not as active and brought only isolated thunderstorms and light rain. From 16th to 21st a spell of fine and hot weather prevailed as winds moderated and veered to a southerly direction. On 22nd winds turned southwesterly bring thundery showers in late morning. This unsettled period continued as another trough crossed the coast the next day and lingered for days giving rise to active development of rain clouds in the vicinity of Hong Kong. Squally thunderstorms occurred on the mornings of 23rd and 24th and rainy weather persisted to 26th. This period brought over 200 mm of rain to the Eastern New Territories. A northwesterly airstream associated with the development of a frontal depression to the east of Taiwan brought drier air and the weather improved markedly on 27th. During the following two days, unseasonably dry weather, with relative humidity below 50 percent prevailed. The month's high of 31.7°C was recorded on 28th under bright sunny conditions. Towards the end of the month maritime air returned to moisten the atmosphere and increase cloudiness on 30th. The month ended with an active southwest monsoon bringing fresh, gusty winds and an outbreak of severe squally thunderstorms early on 31st. The affected the eastern New Territories and the northern part of Hong Kong Island.

Mean daily temperature	**26.0°C**	**(+0.1°C)**
Rainfall (provisional)	**338.4 mm**	**(107 %)**

Meeting Reviews

Annual Meeting 1993

Venue: Royal Observatory, Kowloon

Date: 13 March, 1993

Twenty seven members and two observers participated in the Annual Meeting of the Society held at 12 noon on Saturday 13 March, 1993 at the Royal Observatory, Nathan Road, Kowloon.

The outgoing Chairman, Dr. Bill Kyle, welcomed members and guests to the AGM and thanked the members of the 1992-93 Executive Committee for their hard work and the members of the Society for their support during the year. He then presented his annual report for 1992-93 which highlighted the following points.

On 28th February, 1993 membership of the Society stood at 190, comprising 107 Fellows, 57 Associate Members, 14 Student Members and 12 Corresponding Members. This total represents an increase of about 10 percent over the previous year. Although this increase is less than in previous years it is still a good sign of a growing Society. The still small number of Student Members however, suggests that greater effort is needed to recruit and keep this category of membership.

During the year various activities of scientific and technical interest to members and their guests were organized. These included three lectures in the Special Topics Lecture Series, two Research Forums, one on the topic of "Remote Sensing" and a second on the topic of "Short Term Climate Fluctuation", and a Joint Seminar with the Hong Kong University of Science and Technology Research Centre. A Seminar was also organized at the request of McDonald's Restaurants (Hong Kong) Ltd.

Some members of the Society also contributed papers to the Association of Southeast asian Institutions of Higher Learning Seminar on "The Role of ASAIHL in Combatting Health Hazards of Environmental Pollution", organized by The University of Hong Kong in connection with its 80th Anniversary celebrations.

By far the most important event of the year was the "Second International Conference on East Asia and Western Pacific Meteorology and Climate" held from 7 to 10 September, 1992 at Hong Kong Baptist College. The Conference was sponsored by the Society and supported by the University Corporation for Atmospheric Research, USA, K.C. Wong Education Foundation Ltd., Hong Kong and Wei Lun Foundation Ltd., Hong Kong. Altogether there were about 100 attendees from meteorology and related disciplines of whom 80 were invited/registered participants who met to share their knowledge and to exchange their research experiences through paper presentations and discussions.

During the year one issue of the Hong Kong Meteorological Society Bulletin, Volume 2, Number 2 was published by the Editorial Board.

As we are still a small Society in terms of numbers the considerable workload that the organization of these activities have placed on a few people warrants our commendation for their efforts. The remarkable success of the Conference has provided the Society with a higher profile on the international stage and we are justly proud of our ability to host such an outstanding event.

The Hon. Treasurer, Mr. Y.K. Chan, then presented the audited accounts of the Society for the year. These were adopted unanimously.

Election of Office Bearers of the Society, and appointment of the Honorary Legal Advisor and Honorary Auditor produced the following results:

Chairman	Dr. W.J. Kyle
Vice-Chairman	Dr. S.C. Kot
Hon. Secretary	Ms. Olivia S.M. Lee
Hon. Treasurer	Mr. Y.K. Chan
Committee	Dr. J.C.L. Chan
	Ms. Julie Evans-Dowsley
	Mr. C.Y. Lam
	Dr. C.N. Ng
	Mr. Y.S. Sin
Hon. Legal Advisor	Ms. Venus Choy
Hon. Auditor	Mr. J.C.T. Wu

The meeting agreed to continue waiver of the Entry Fee for all those who submit their application to join the Society in 1993-94 as this policy encouraged growth in membership. The following annual subscriptions were also adopted:

HK$150	for Fellow
HK$100	for Associate Member
HK$ 50	for Student Member
US$ 20	for Corresponding Member
HK$500	for Institutional Member

Research Forum 7

Venue: Royal Observatory, Kowloon

Date: 13 March, 1993

Subject: Acquisition and Application of Hydrological Data

A seventh research forum was held at the Royal Observatory, Kowloon with the theme of the *Acquisition and Application of Hydrological Data*. The forum was organized by Mr. Y.K. Chan of the Royal Observatory Hong Kong who also chaired both sessions.

Two papers were delivered in the first session as listed.

HYDROLOGICAL DATA ACQUISITION AND ANALYSIS AT THE ROYAL OBSERVATORY

by Ms. C.C. Lam,
Royal Observatory Hong Kong

THE INFLUENCE OF METEOROLOGY ON APPLIED HYDROLOGY AND WATER QUALITY

by Dr. M.R. Peart, Department of Geography and Geology, The University of Hong Kong

Following a break for refreshments two more papers were delivered in a second session as listed.

A REAL-TIME FLOOD FORECASTING SYSTEM FOR HONG KONG

by Mr. Nick Townsend, Binnie-Maunsell Consultants, Hong Kong

EXTRACTION OF WATER FROM CLOUDS: AN OCCULT PRECIPITATION EXPERIMENT AT TAI MO SHAN

by Dr. W.J. Kyle, Department of Geography and Geology, The University of Hong Kong

香港氣象學會

HKMetS BULLETIN, Vol. 3, Number 2, 1993

HONG KONG METEOROLOGICAL SOCIETY

BULLETIN

CONTENTS

Editorial 2

Recent Sea-Level Changes in Hong Kong and Their Implications 3
Wyss W.S. Yim

Diurnal Atmospheric Secondary Circulations over Hong Kong 9
Mickey Man-Kui Wai

The First Radioactivity and Ozone Soundings in Hong Kong 21
C.M. Shun & K.S. Leung

News and Announcements 28

Hong Kong Weather Reviews 39

Meeting Reviews 45